AD_____

Award Number: DAMD17-01-1-0178

TITLE: Anti-Angiogenesis Therapeutic Indicators in Breast Cancer

PRINCIPAL INVESTIGATOR: Min-Ying L. Su, Ph.D.

CONTRACTING ORGANIZATION: University of California, Irvine
Irvine, California 92697-1875

REPORT DATE: August 2004

TYPE OF REPORT: Final

PREPARED FOR: U.S. Army Medical Research and Materiel Command
Fort Detrick, Maryland 21702-5012

REPORT DOCUMENTATION PAGE

Form Approved
OMB No. 074-0188

1. AGENCY USE ONLY (Leave blank)	2. REPORT DATE	3. REPORT TYPE AND DATES COVERED
	August 2004	Final (2 Jul 2001 - 1 Jul 2004)

4. TITLE AND SUBTITLE
Anti-Angiogenesis Therapeutic Indicators in Breast Cancer

5. FUNDING NUMBERS
DAMD17-01-1-0178

6. AUTHOR(S)
Min-Ying L. Su, Ph.D.

7. PERFORMING ORGANIZATION NAME(S) AND ADDRESS(ES)
University of California, Irvine
Irvine, California 92697-1875

E-Mail: msu@uci.edu

8. PERFORMING ORGANIZATION REPORT NUMBER

9. SPONSORING / MONITORING AGENCY NAME(S) AND ADDRESS(ES)
U.S. Army Medical Research and Materiel Command
Fort Detrick, Maryland 21702-5012

10. SPONSORING / MONITORING AGENCY REPORT NUMBER

11. SUPPLEMENTARY NOTES
Original contains color plates: All DTIC reproductions will be in black and white.

12a. DISTRIBUTION / AVAILABILITY STATEMENT
Approved for Public Release; Distribution Unlimited

12b. DISTRIBUTION CODE

13. ABSTRACT (Maximum 200 Words)

This project was proposed to study therapeutic indicators for anti-angiogenic therapy. Two different animal tumor models were studied, R3230 AC adenocarcinoma and carcinogen ENU induced tumors. Longitudinal MRI studies were performed before and during therapy to monitor the changes occurring over the entire treatment period. Immunohistochemical analysis was performed to measure 4 molecular markers p53, TSP-1, VEGF and factor VIII microvessel density in pre-treatment and post-treatment specimens. ENU induced tumors came with different types, thus could simulate the wide variation of human breast cancer. However, the tumor also showed a very complicated response pattern. All MRI markers and IHC markers were correlated with final treatment outcome. Unlike in humans, the early volumetric changes did not predict outcome. The contrast enhancement kinetics measured using the blood pool agent Gadomer-17 may provide an indication for therapy response. The vascular volume measured by Gadomer-17 decreased in responder, and increased in non-responders. Also the baseline vascularity measured by Gaomer-17 was associated with future response, possibly due to a higher blood supply thus more delivery of therapeutic agents. The developed methodology is currently applied in human studies, and that is expected to yield more interesting results in understanding chemotherapy induced changes.

14. SUBJECT TERMS	15. NUMBER OF PAGES
Breast cancer	43
	16. PRICE CODE

17. SECURITY CLASSIFICATION OF REPORT	18. SECURITY CLASSIFICATION OF THIS PAGE	19. SECURITY CLASSIFICATION OF ABSTRACT	20. LIMITATION OF ABSTRACT
Unclassified	Unclassified	Unclassified	Unlimited

Table of Contents

(4) Introduction

Anti-angiogenic therapy is a promising alternative for treatment of cancer, also it may be used as maintenance therapy to prevent metastasis or recurrence. While 60% of the approximately 186,000 annual cases of breast cancer now present as node negative, 30% of these cases will recur after local therapy. Although adjuvant chemotherapy has been demonstrated to improve survival in node negative breast cancer, it is still unclear how best to identify those patients whose risk of metastatic disease exceeds their risk of significant therapeutic toxicity. On the other hand, for treatment of locally advanced disease, anticancer chemotherapy has produced only modest gains. Newer therapeutic strategies are greatly needed. Anti-angiogenic therapy maybe used to augment the efficacy of the traditional cytotoxic therapeutic agents. Furthermore, a new line of therapy that has a less side toxicity effect is definitely needed to provide the patients with more options for treatment. Because angiogenesis appears to play an important role in the disease progression, anti-angiogenic agents may have a great potential for treating breast cancer.

While the efficacy of traditional therapeutics has been determined by measuring tumor response and patient survival, these newer approaches may prolong life and improve symptoms by stabilizing tumor progression rather than by causing tumor shrinkage. It is therefore necessary to develop improved endpoints that can determine the clinical activity of these agents during their development. In this project we used in vitro and in vivo strategies to measure the potential efficacy of anti-angiogenic compounds in order to facilitate their clinical development. Two breast cancer models, R3230 AC adenocarcinoma and carcinogen N-ethyl-N-nitrosourea(ENU) induced mammary tumors will be used, and two drugs known to have anti-angiogenesis effect, taxotere and thalidomide, will be used to treat cancers. We will measure the therapy induced changes using the in vivo magnetic resonance imaging and the in vitro immunohistochemistry. Dynamic contrast enhanced MRI has been shown as a non-invasive means to measure the vascular characteristics in tumors. We will apply this technique to measure the longitudinal structural and vascular changes taking place in tumors following treatment. While these structural and vascular changes observed by MRI are macroscopic, they are governed by the underlying biological changes, e.g. the decrease of microvessel density and changes of other angiogenic markers. The vascular changes measured by MRI will be correlated with the neovessel density count (obtained by immunohistochemistry with CD105 staining) and the angiogenesis index (AI, constituting 3 angiogenic markers, p53, TSP-1, CD31) and expression level of VEGF.

After completion of this pilot study we expect to achieve three goals: (1) to assess the feasibility of using these two animal models for testing the efficacy of other potential anti-angiogenic compounds, (2) to identify other therapeutic indicators rather than tumor shrinkage (immunohistochemical markers or MRI cellular and vascular parameters) for determination of therapeutic efficacy, (3) to find early therapeutic indicators which will predict the final outcome.

(5) Body

Five specific aims were proposed. First we will establish the tumor models. For each tumor, when the size reaches 1.0 cm the baseline MRI study will be performed. After the MRI study core needle biopsy will be performed to obtain tissue specimens for analysis of baseline angiogenic biomarkers. Then the tumor will receive treatment. Several MRI studies will be performed to follow the longitudinal changes. At the conclusion of the study the animal will be sacrificed, and the tumor excised for measures of post-treatment angiogenic biomarkers.

Aim 1. Establish the R3230 AC adenocarcinoma and ENU induced mammary tumor models.

Aim 2. Perform the baseline dynamic contrast enhanced MRI before administration of therapeutic drugs to measure the pre-treatment characteristics of tumors.

Aim 3. Perform core needle biopsy to obtain cancer specimens for evaluation of baseline angiogenic activity using immunohistochemical analysis.

Aim 4. Apply dynamic contrast enhanced MRI to monitor the longitudinal volumetric, cellular and vascular changes taking place in tumors following therapy.

Aim 5. Perform immunohistochemical studies to measure the CD105 neovessel density, VEGF, and the angiogenesis index (AI) markers in tumors for assessment of anti-angiogenic effects.

The R3230 studies were completed in Yr-01. At beginning of this project 53 rats were injected with carcinogen ENU, and 46 mammary tumors were found. The MRI studies were completed in Yr-02. During last year (no-cost extension) immunohistochemical studies were performed on all ENU specimens, including pre-treatment biopsy samples and post-treatment tumors. The results are summarized below. In addition to these specified studies, specimens from another study were available to this project. Immunohistochemical analysis was also performed, and the data have been described in previous reports. Here all previously reported results are briefly summarized, and new results are described in details. The entire publications related to this project are enclosed in the appendix.

Longitudinal Taxotere Chemotherapy Treatment Induced Vascular and Structural Changes Measured by Dynamic Enhanced MRI

in "Proc., 10th ISMRM Annual Meeting, Hawaii, 2002" p2131.

Abstract: Chemotherapy induced longitudinal vascular changes taking place during the growth of an animal tumor, R3230 AC adenocarcinoma were investigated using two contrast agents with different molecular weights, Gd-DTPA and Gadomer-17. Treated animals were separated into responders and partial-responders according their viable growth rate 3 weeks after the therapy. In responders a decrease in the vascular volume as well as in the vascular permeability were observed at 2-week post-therapy compared to 1-week's, whereas in controls an increase in both the vascular volume and permeability were observed at 2-week's compared to 1-week's as measured by Gadomer-17 using a pharmacokinetic model on a pixel-by-pixel basis, suggesting that vascular changes assessed by Gadomer-17 could serve as a tumor treatment monitor.

Characterization of Carcinogen ENU Induced Benign and Malignant Mammary Tumors in Rats: Volumetric Growth Rates, Contrast Enhancement Kinetics, and Longitudinal Monitoring

"Proc., 10th ISMRM Annual Meeting, Hawaii, 2002" p2180.
Abstract: The carcinogen ENU could induce malignant tumors of various nuclear grades and different types of benign tumors, thus it can serve to investigate the sensitivity and specificity of experimental diagnostic agents for differential diagnosis and tumor staging. However, whether it can be used for studies of recurrence or metastasis has rarely been studied. We measured the volumetric growth rate and the enhancement kinetics of Gd-DTPA and Gadomer-17 for each tumor, and differences between malignant and benign tumors were investigated. Each tumor was surgically removed and the rats were kept for longitudinal monitoring for recurrence, development of other tumors, and metastasis.

Quantitative Vascular Density Assessed by a Semiautomatic Histological Method in Comparison with MRI Enhancements in Carcinogen Induced Benign and Malignant Mammary Tumors in Rats
in "Proc., 10th ISMRM Annual Meeting, Hawaii, 2002" p2108.
Abstract: The development of therapeutic efficacy markers for anti-angiogenic or anti-vascular therapy is in great need. Assessment of microvascular density by immunohistochemical staining is the most commonly used technique. Imaging can provide a thorough sampling, but to date there is not a suitable agent and technique whose accuracy has been validated. In this study, we developed a semi-automatic histological analysis method to quantitatively measure the cross-sectional area of vessels in carcinogen ENU induced benign and malignant tumors. The results were compared to enhancements measured by three contrast agents, Gd-DTPA, Gadomer-17, and albumin-Gd-DTPA.

Characterization of Angiogenesis in The Carcinogen ENU Induced Benign And Malignant Mammary Tumor Model
in "Proc., 11th ISMRM Annual Meeting, Toronto, 2003"
Abstract: Angiogenesis in carcinogen ENU-induced benign and malignant tumor models were studied with dynamic contrast enhanced MRI using two contrast agents (Gadodiamide and Gadomer-17). The tumors were then excised for immunohistochemical (IHC) staining to measure expression of angiogenic biomarkers, including mutant p53, TSP-1, VEGF, and Factor VIII microvessel density. Benign and malignant tumors had distinct contrast enhancement kinetics. Malignant tumors had a higher microvessel density than benign tumors. MRI and IHC may provide different aspects (macroscopic and microscopic) complementing each other for assessment of tumor angiogenesis.

Monitoring Chemotherapy Induced Changes in the Carcinogen ENU Induced Infiltrating Ductal Adenocarcinoma and Non-Infiltrating Papillary Adenocarcinoma by Longitudinal MRI studies
Abstract
The wide variation of tumor types and grades induced by ENU were used to simulate human breast tumors. Their response to chemotherapy (Taxotere) was studied. Longitudinal MRI was applied to measure tumor volume and contrast enhancement kinetics of Gd-DTPA-BMA and Gadomer-17. Infiltrating ductal adenocarcinomas showed mixed response, fibroadenomas did not respond well, and all 3 non-infiltrating papillary adenocarnoma were stabilizers. The baseline Gadomer-17 enhancements at 1-min and 2-min revealed a significant difference between +/- tumor growth groups at week-1, suggesting that tumors with a higher vascularity measured by Gadomer-17 had a better response, possibly due to more drug delivery.

Purpose

It is well known that carcinogen ENU can induce benign and malignant tumors. In this study we utilized this wide variation of tumor types and tumor grades to simulate human breast cancer, and studied their response to chemotherapy (Taxotere). Longitudinal MRI was applied to measure the tumor volume and the contrast enhancement kinetics of a small extracellular agent Gd-DTPA-BMA and a medium size blood pool agent Gadomer-17. We investigated whether the vascular parameters measured by contrast enhanced MRI at an early time can differentiate responders from non-responders at later times, thus to predict therapy outcome.

Methods

53 Sprague-Dawley rats were injected with 90 mg/kg carcinogen ENU (N-ethyl-N-nitrosourea). Forty seven mammary tumors appeared within 9 months, and 35 tumors grew to 1.0 cm for the MRI study, which included 23 infiltrating ductal adenocarcinoma (IDC), 3 non-infiltrating papillary adenocarcinoma (NPC), 7 fibroadenoma (FA), 1 Sclerosing adenosis, and 1 papilloma. The baseline MRI was conducted when the tumor reached 1 cm. The imaging protocol included a T2-weighted sequence for volumetric measurement, and the dynamic study using a small molecular weight agent Gd-DTPA-BMA (®Omniscan, 0.1 mmol/kg), followed by an intermediate molecular weight agent Gadomer-17 (0.05 mmol/kg, provided by Schering AG, Germany). After the MRI study was completed the rats received i.v. injection of 4 mg/kg Taxotere. Three follow-up MRI studies were performed, once per week (noted as W1, W2, and W3). The rats continued to receive weekly Taxotere treatment after each MRI study. The volume of each tumor was measured, and depending on the volumes at W3 compared to the baseline, the tumors were separated into responders (volume decreased by 50%), non-responders (volume increased by 50%), and stabilizer (others). Also, the response at each time point compared to the baseline was analyzed. The MRI enhancement parameters (at 30 sec, 1-min, and 2-min) and the K21 decay rate were used to investigate whether any of these parameters themselves, or the changes compared to the previous time measures, can be used to differentiate responders from non-responders at a later time.

Results

Among these 35 tumors, 29 tumors (20 IDC, 3 NPC, 4 FA, 1 adenosis, and 1 papilloma) have completed the longitudinal study at 4 time points. According to the tumor volume at the end of week-3 compared to the baseline (noted as GR), the tumor was classified into responder ($GR < 0.5$), stabilizer ($0.5 < GR < 1.5$), and non-responder ($GR > 1.5$). Of the 20 IDC, 9 were responders, 5 were stabilizers, and 6 were non-responders. Interestingly all 3 NPC were stabilizer. Three fibroadenomas were non-responders and only one FA was a responder. Figure 1 shows the T2-weighted images and the contrast enhancement kinetics from an IDC which showed a consistent regression. Figure 2 shows another IDC which grew larger over time. However, not every tumor was responding consistently. Given the complicated response pattern, the statistical analysis was only performed for IDC and the response at each time point was analyzed separately. Tumor size at week-1 compared to the baseline was calculated, and separated into +/- growth groups. Among all 8 MRI parameters, the baseline Gadomer-17 enhancements at 1-min and 2-min at baseline showed a significant difference ($p < 0.05$, Wilcoxon rank-sum tests) between the 2 groups with +/- growth at week-1. The same analysis was applied at week-2 and week-3, but no MRI parameters revealed a significant difference between different growth groups at week-2 and week-3.

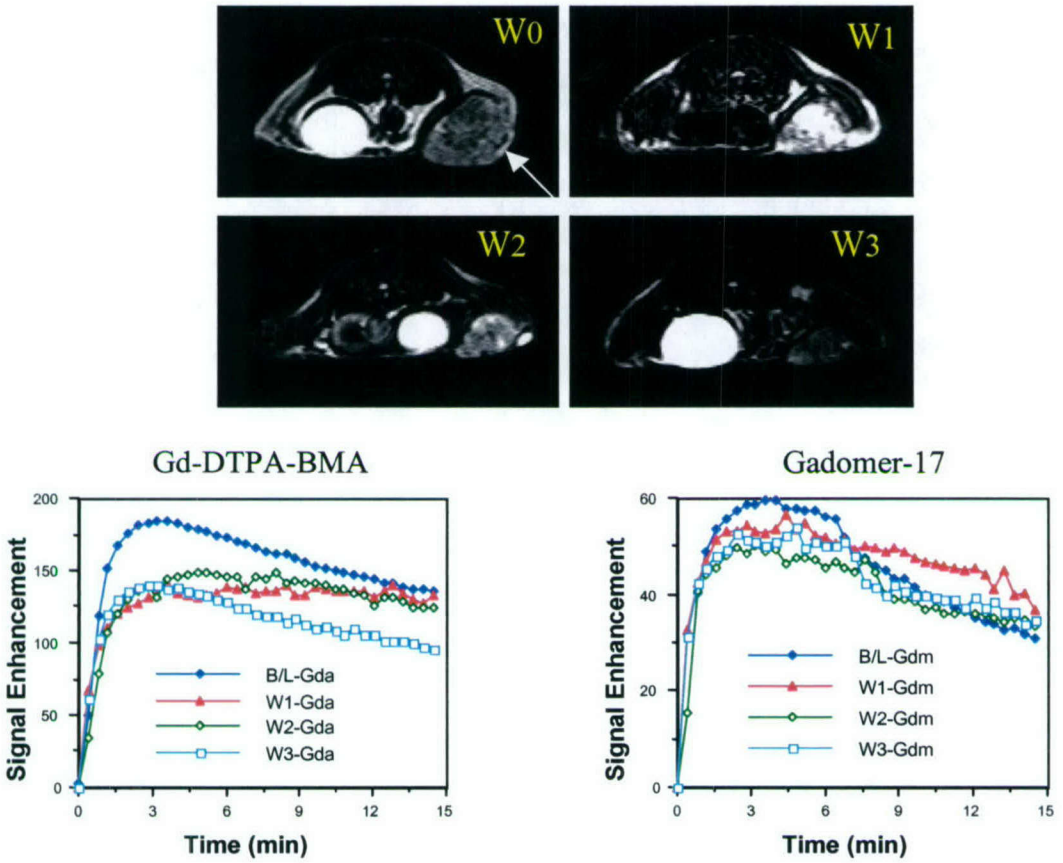

Figure 1: The T2-weighted image, and the enhancement kinetics measured by Gd-DTPA-BMA and Gadomer-17 in one responder tumor (infiltrating ductal adenocarcinoma). The tumor showed continuous regression over time. The kinetics measured by Gd-DTPA-BMA showed reduced intensity after the first treatment, and the pattern of the curve became more flattened (i.e. no wash-out).

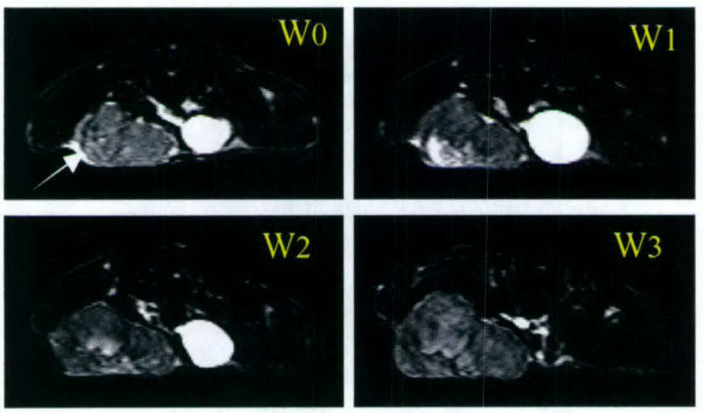

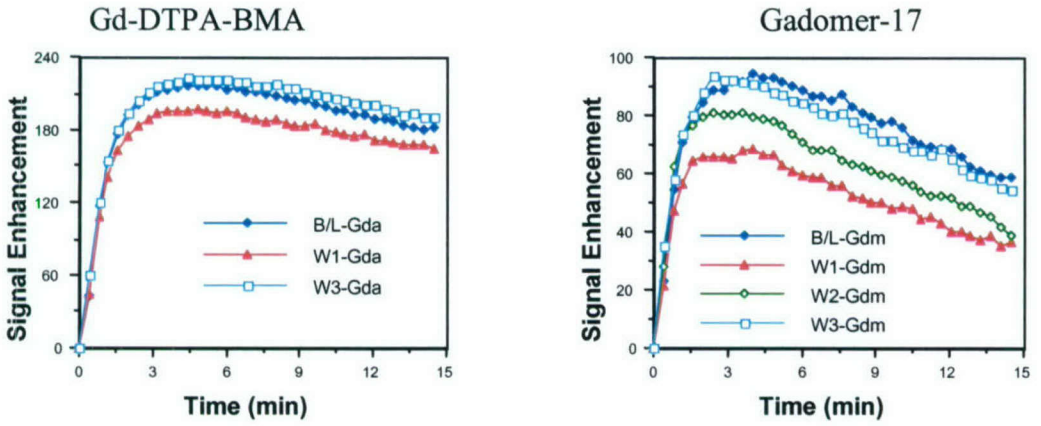

Figure 2: The T2-weighted image, and the enhancement kinetics measured by Gd-DTPA-BMA and Gadomer-17 in one non-responder tumor (infiltrating ductal adenocarcinoma). The tumor grew larger and larger over time. The Gd-DTPA-BMA kinetics were similar over time, and the Gadomer-17 kinetics showed a great reduction at Week-1 then recovered to the baseline level at Week-3.

Discussion

The volumetric changes and contrast enhancement changes in ENU induced tumors receiving Taxotere were measured by longitudinal MRI. ENU induced benign and malignant tumors (came with 2 major types, infiltrating ductal adenocarcinoma, and non-infiltrating papillary adenocarcinoma simulating in-situ cancers). Among all tests, only the baseline Gadomer-17 enhancements at 1-min and 2-min revealed a significant difference between IDC's which grew bigger at week-1 versus those which shrank at week-1. This maybe interpreted as that tumors with a higher vascularity measured by Gadomer-17 had a better response (shrinkage), possibly due to more drug delivery. The data also indicated that although ENU induced tumors came with a large variation, they also showed different responses to therapy. Although ENU induced tumors may simulate the variety in human breast cancer, but it may not be a good tumor model for drug response testing.

Immunohistochemical Staining in pre-treatment Biopsy samples and post-treatment specimens

Purpose

In addition to MRI which was used to accurately measure the tumor volume and magnitude of contrast enhancements, molecular markers were used to measure the underlying molecularbiology of angiogenesis. After the baseline MRI study was completed, biopsy was performed to obtain tissue samples, then chemotherapy was administered. After the animal completed 3 cycles chemotherapy, the animal was euthanized, and the tumors were excised. The pre-treatment biopsy samples and the post-treatment tumor specimens were stained using immunohistochemical methods to measure the microvessel density, and the expression level of p53, TSP-1 and VEGF. The results in pre-treatment and post-treatment samples were compared, also the differences in different tumors were investigated.

Methods

Four IHC markers were studied, p53 (using Santa Cruz SC6243), Factor VIII microvessel density (using Zymed 180018 antibody), thrombopondin-1 (using Labvision MS421 antibody), and VEGF (using Santa Cruz SC7269 antibody). The intensity of p53 and VEGF staining was scored as follows: negative when less than 5% of tumor cells display staining, 1+ when the intensity of staining is mild, 2+ moderate, 3+ intense and equal to positive control, 4+ when intensity is greater than positive control. VEGFand p53 Histoscores were calculated by multiplying % of positive cells

by the intensity of staining plus 1 [Histoscore = % positive cells x (intensity + 1)]. Vascular counts were determined by light microscopy under 200x magnification. Three areas where the highest number of discreet microvessels were stained were chosen by a pathologist, and any immunoreactive endothelial cell that is separate from adjacent microvessels will be considered as a "countable" vessel. For TSP-1, image analysis using the CAS 200 system (Becton Dickinson, San Jose, CA) was performed to quantify the staining intensity of the TSP1 marker positive cell populations. Values were converted to the product of positive area and positive stain expressed as optical density (O.D.) units using CAS 200 software.

Results

Figures 3-6 show the IHC staining slides of Factor VIII vessel density using Zymed 180018 antibody, and VEGF using Santa Cruz SC7269 antibody in 4 different tumor types, 2 malignant-infiltrating ducal carcinoma and papillary adenocarcinoma, and 2 benign-fibroadenoma and adenosis. The two malignant tumors had higher Factor VIII microvessel densities than the two benign tumors. Ductal adenocarcinoma had the highest VEGF, and the fibroadenoma also had a high VEGF. All ENU tumors had positive p53 staining.

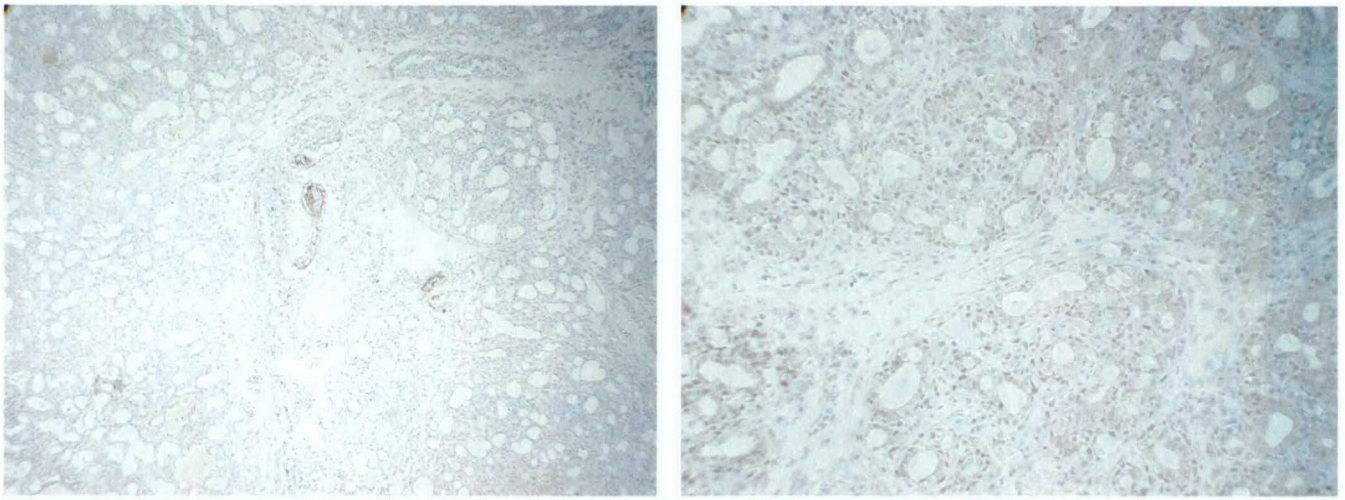

Figure 3: The immunohistochemical staining for Factor VIII (using Zymed 180018 antibody, left) and VEGF (using Santa Cruz SC7269 antibody, right) in one infiltrating ductal carcinoma (IDC). The vessel density was 114/200x field, and VEGF staining showed 100% positive cells with 2-3+ intensity.

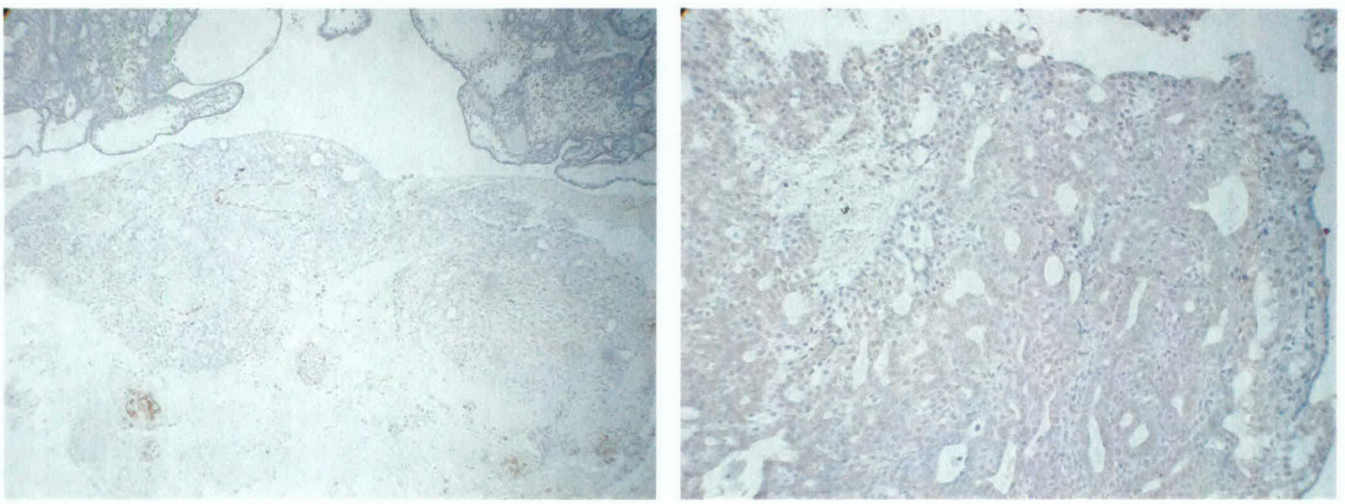

Figure 4: The immunohistochemical staining for Factor VIII (using Zymed 180018 antibody, left) and VEGF (using Santa Cruz SC7269 antibody, right) in one papillary adenocarcinoma (PAC). The vessel density was 106/200x field, and VEGF staining showed 30% positive cells with 1+ intensity.

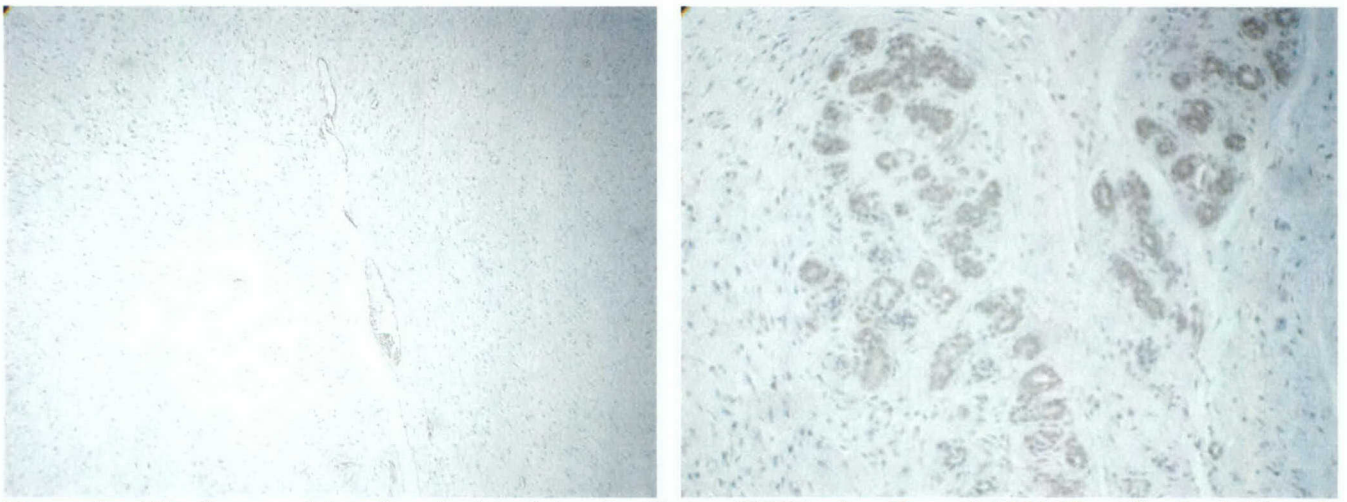

Figure 5: The immunohistochemical staining for Factor VIII (using Zymed 180018 antibody, left) and VEGF (using Santa Cruz SC7269 antibody, right) in one benign fibroadenoma (FA). The vessel density was 90/200x field, and VEGF staining showed 80% positive cells with 3+ intensity.

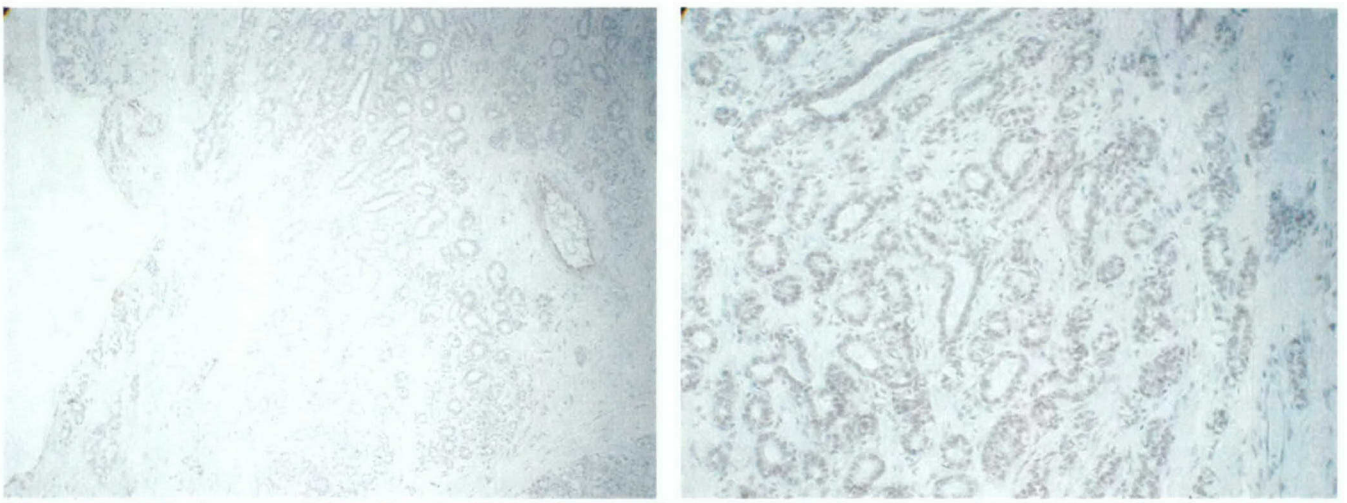

Figure 6: The immunohistochemical staining for Factor VIII (using Zymed 180018 antibody, left) and VEGF (using Santa Cruz SC7269 antibody, right) in one benign adenosis (ADNS). The vessel density was 76/200x field, and VEGF staining showed 50% positive cells with 2+ intensity.

The results in pre-treatment biopsy samples and post-treatment specimens are shown in Figures 7-9. Majority of ENU induced tumors were IDC, and 20 of them completed 3 cycles treatment. The response was assessed based on the final volume compared to the baseline volume. Of these 20 IDC, 11 were responders, 5 were stabilizer, and 6 were non-responders. All 3 PAC were stabilizer, and 3 of 4 fibroadenoma were non-responders. The data from these 5 groups are shown in the figure, including IDC responder (IDC_Res), IDC stabilizer (IDC_Stbl), IDC non-responder (IDC_NonR), PAC stabilizer (PAC_Stbl), and fibroadenoma non-responder (FA_NonR). The individual responses of 9 tumors in the IDC responders are shown in Figure 10.

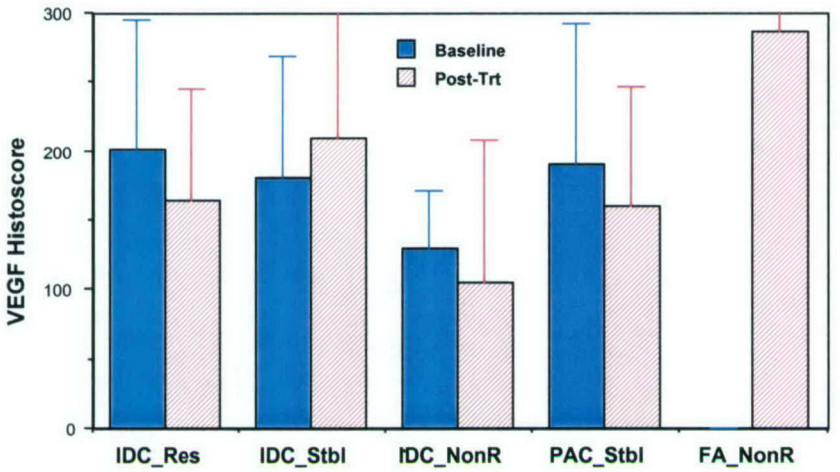

Figure 7: The VEGF histoscore, defined as [% positive cells x (staining intensity+1)], measured from the biopsy samples taken in the baseline study before treatment and from the post-treatment specimens. The data in 5 groups are shown, IDC responder (IDC_Res), IDC stabilizer (IDC_Stbl), IDC non-responder (IDC_NonR), PAC stabilizer (PAC_Stbl), and fibroadenoma non-responder (FA_NonR). The pre-treatment IHC data for FA group were not available. Error bars show the standard deviation. The baseline measures were not significantly different between groups. The IDC_NonR group had a lower VEGF histoscore compared to others, but not significant. Very high deviation was noted. Although some changes were seen after treatment, but not significance.

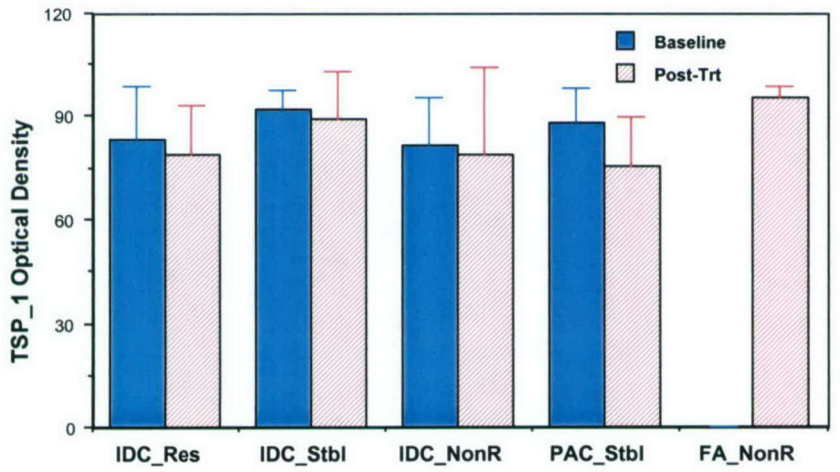

Figure 8: The TSP-1 optical density measured from the biopsy samples taken in the baseline study before treatment and from the post-treatment specimens. Error bars show the standard deviation. The baseline measures were not significantly different between groups, and no significant changes were noted after treatment.

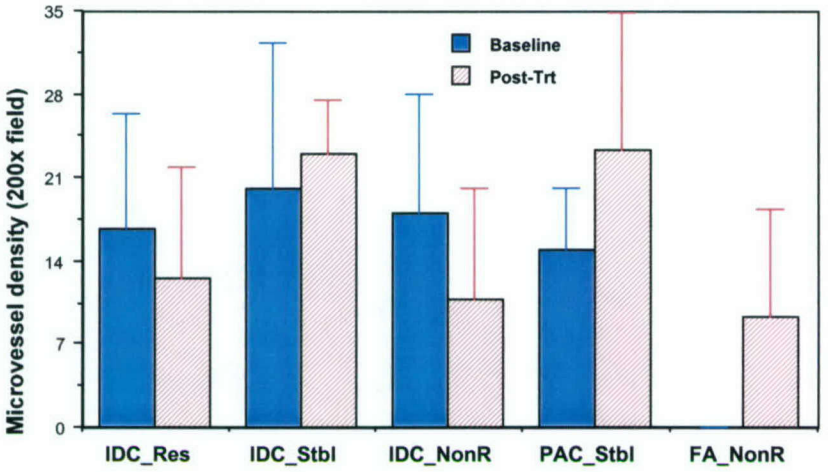

Figure 9: The Factor VIII vessel density measured from the biopsy samples taken in the baseline study before treatment, and from the post-treatment specimens. Error bars show the standard deviation. The baseline measures were not significantly different between groups. Although some changes were seen after treatment, not reaching the significance level.

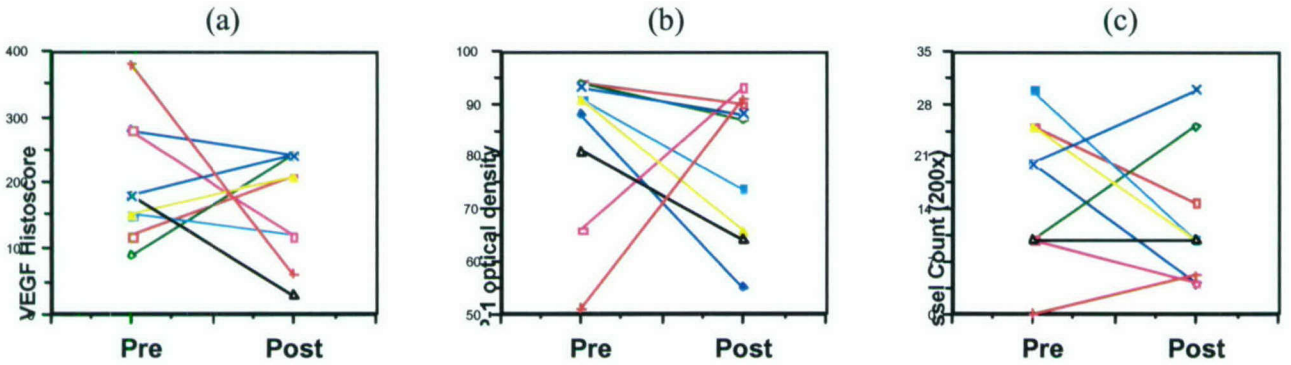

Figure 10: The changes of VEGF histoscore (a), TSP-1 optical density (b) and Factor VIII vessel count in 200x field (c) in the post-treatment specimen compared to the pre-treatment biopsy sample, for the 9 individual tumors in the IDC_Responder group. Some tumors showed increase and some showed decrease, thus no consistent changes were noted.

Two statistical analyses were performed, first to investigate whether the baseline IHC measures were different between tumors in different response groups, then to investigate whether the changes after therapy were correlated with responses. The results did not reveal significant differences in baseline IHC measures between groups, also there was not significant post-therapy changes between groups. It is known that tissue sampling is a major problem in any type of molecular analysis. That may be one reason to account for the insignificant results. Another reason may be the complicated response pattern as reported previously. Some tumor would grow larger then regress, and some would regress first then grow larger. In the current analysis the overall treatment outcome was determined based on the volume at week-3 compared to the baseline, the IHC data may also be analyzed with respect to responses at week-1 and week-2, as for the analysis of MRI data.

(6) Key Research Accomplishments

- Carried out magnetic resonance imaging studies to monitor the taxotere treatment-induced effects in R3230AC and ENU induced tumors
- Performed immunohistochemical studies to stain p53, TSP-1, Factor VIII, and VEGF in rat tissues. The specimens available from a previous study consisting of various tumor types, and the current study before and after chemotherapy were studied.
- Correlate MRI data and the IHC marker data with the tumor types and the response to chemotherapy.

(7) All publications related to this project

- Two journal papers were published.
- Six conference papers were presented.

Journal Paper:

Min-Ying. Su, Hon Yu, Jr-Yuan Chiou, Jun Wang, John P. Fruehauf, Orhan Nalcioglu, Rita S. Mehta, and Choong Hyun Baick. Measurements of Volumetric Changes and Vascular Changes with Dynamic Contrast Enhanced MRI for Cancer Therapy Monitoring. Technology in Cancer Research and Treatment, **1**(6): 479-488, 2002.

M. Samoszuk, L. Leonor, F. Espinoza, P. M . Carpenter, O. Nalcioglu, and M.-Y. Su. Measuring microvascular density in tumors by digital dissection. Analytical and Quantitative Cytology and Histology **24**(1):15-22, 2002.

Conference Abstracts:

M-Y. Su, M. J. Hamamura, H. Wang, H. J. Yu, J. Wang, P. M. Carpenter, O. Nalcioglu. Monitoring Chemotherapy Induced Changes in the Carcinogen ENU Induced Infiltrating Ductal Adenocarcinoma and Non-Infiltrating Papillary Adenocarcinoma by Longitudinal MRI Studies. "Proc., 12th ISMRM Annual Meeting, Kyoto, Japan, 2004" p2373.

Min-Ying Su, Hon Yu, Jun Wang, Phillip Carpenter, John Fruehauf, and Orhan Nalcioglu, "Characterization of Angiogenesis in The Carcinogen ENU Induced Benign And Malignant Mammary Tumor Model". in "Proc., 11th ISMRM Annual Meeting, Toronto, 2003"

Min-Ying Su, Hon Yu, Jun Wang, Orhan Nalcioglu, "Characterization Of Angiogenesis in The Carcinogen ENU Induced Benign And Malignant Mammary Tumor Model" Second Era of Hope meeting (Department of Defense Breast Cancer Research Program Meeting), Orlando, FL, 2002

Min-Ying Su, Michael Samoszuk[2], Leonard Leoner, Phillip M. Carpenter[2], and Orhan Nalcioglu, Quantitative Vascular Density Assessed by a Semiautomatic Histological Method in Comparison with MRI Enhancements in Carcinogen Induced Benign and Malignant Mammary Tumors in Rats. . in "Proc., 10th ISMRM Annual Meeting, Hawaii, 2002" p2108.

Hon Yu, Min-Ying Su, Jun Wang, and Orhan Nalcioglu, Longitudinal Taxotere Chemotherapy Treatment Induced Vascular and Structural Changes Measured by Dynamic Enhanced MRI. in "Proc., 10th ISMRM Annual Meeting, Hawaii, 2002" p2131.

Hon Yu, Min-Ying Su, Jun Wang, Phillip M. Carpenter[2], and Orhan Nalcioglu, Characterization of Carcinogen ENU Induced Benign and Malignant Mammary Tumors in Rats: Volumetric Growth Rates, Contrast Enhancement Kinetics, and Longitudinal Monitoring. in "Proc., 10th ISMRM Annual Meeting, Hawaii, 2002" p2180.

(8) Research personnel during the entire project years

Min-Ying Su, PhD	PI
Orhan Nalcioglu, PhD	Investigator
John Fruehauf, MD PhD	Investigator
Tugan Muftuler, PhD	Investigator
Jun Wang, MD	Post-doc
Changqing Chen, MD	Post-doc
Huali Wang, MD PhD	Post-doc
Hon Yu	Graduate student
Mark Hamamura	Graduate student
Leonard Leoner	Staff Research Assistant
Nabil Saba	MRI system engineer
Liqun Chang	Animal technician
Mine Demir	Project coordinator
Atiye Muftuler	Project coordinator

(9) Conclusions

This project was proposed to study therapeutic indicators for anti-angiogenic therapy. Two different animal tumor models were studied, R3230 AC adenocarcinoma and carcinogen ENU induced tumors. Longitudinal MRI studies were performed before and during therapy to monitor the volumetric and vascular changes occurring over the entire treatment period. Two different MR contrast agents, one clinically approved agent and one medium-sized blood pool agent Gadomer-17, were used to measure the contrast enhancement kinetics in each MRI study. After the baseline MRI study, biopsy was performed to obtain pre-treatment tissue samples. After completing the therapy, the tumor specimens were also obtained for immunohistochemical analysis. Four molecular markers p53, TSP-1, VEGF and factor VIII microvessel density were studied. The longitudinal MRI volumetric and contrast enhancement data and the IHC marker data from pre- and post-treatment tissue samples were correlated with the tumor responses to investigate whether they were associated with, thus could predict, the final treatment outcome.

Three goals were stated in the proposal. Here the results were concluded with respect to each goal.
(1) to assess the feasibility of using these two animal models for testing the efficacy of other potential anti-angiogenic compounds

R3230 AC tumor was a malignant adenocarcinoma in rats. It had a very rapid growth rate, and therapy could only slow down its growth, never regress the tumor. ENU induced tumors came with different types, thus could simulate the wide variation of human breast cancer. However, the tumor also showed a very complicated response pattern, not a steadily progressing, stabilizing, or steadily regressing pattern as in humans. However, that may be due to relatively ineffective therapy used in this study. The response pattern may be better appreciated with a more effective therapy.

(2) to identify other therapeutic indicators rather than tumor shrinkage (immunohistochemical markers or MRI cellular and vascular parameters) for determination of therapeutic efficacy

Among all parameters, including immunohistochemical markers or MRI cellular and vascular parameters, there was not a parameter showing consistent changes, thus none of them could be used to determine therapeutic efficacy. Tumor volume was still the most useful and relevant indicator.

(3) to find early therapeutic indicators which will predict the final outcome.

All MRI markers and IHC markers were correlated with final treatment outcome (as assessed by final volumetric change). Unlike in humans, the early volumetric changes did not predict outcome. The contrast enhancement kinetics measured using the blood pool agent Gadomer-17 may provide an indication for therapy response. In R3230AC tumor, it was shown that the vascular volume measured by Gadomer-17 decreased in responder, and increased in non-responders. In ENU induced tumors it was shown that the baseline vascularity measured from Gaomer-17 contrast enhancement was associated with future response, possibly due to a higher blood supply thus more delivery of therapeutic agents.

(10) Appendices

One new abstract presented at the 12th ISMRM meeting is attached to this report.
M-Y. Su, M. J. Hamamura, H. Wang, H. J. Yu, J. Wang, P. M. Carpenter, O. Nalcioglu. Monitoring Chemotherapy Induced Changes in the Carcinogen ENU Induced Infiltrating Ductal Adenocarcinoma and Non-Infiltrating Papillary Adenocarcinoma by Longitudinal MRI Studies. "Proc., 12th ISMRM Annual Meeting, Kyoto, Japan, 2004" p2373.

One set of all related publications is enclosed.

Monitoring Chemotherapy Induced Changes in the Carcinogen ENU Induced Infiltrating Ductal Adenocarcinoma and Non-Infiltrating Papillary Adenocarcinoma by Longitudinal MRI studies

Min-Ying Su, Mark Hamamura, Huali Wang, Hon Yu, Jun Wang, Philip Carpenter, Orhan Nalcioglu
Center for Functional Onco-Imaging and Department of Pathology, University of California-Irvine, CA 92697-5020, USA

Purpose

It is well known that carcinogen ENU can induce benign and malignant tumors. In this study we utilized this wide variation of tumor types and tumor grades to simulate human breast cancer, and studied their response to chemotherapy (Taxotere). Longitudinal MRI was applied to measure the tumor volume and the contrast enhancement kinetics using two contrast agents (a small extracellular agent Gd-DTPA-BMA, and a medium size blood pool agent Gadomer-17). We investigated whether the vascular parameters measured by dynamic contrast enhanced MRI at an early time can differentiate responders from non-responders at later times, thus to predict therapy outcome.

Methods

53 Sprague-Dawley rats were injected with 90 mg/kg carcinogen ENU (N-ethyl-N-nitrosourea). Forty seven mammary tumors appeared within 9 months after ENU injection, and 35 tumors grew to 1.0 cm for the MRI study, which included 23 infiltrating ductal adenocarcinoma (IDC), 3 non-infiltrating papillary adenocarcinoma (NPC), and 7 fibroadenoma (FA) 1 Sclerosing adenosis and 1 papilloma. The baseline MRI was conducted when the tumor reached 1 cm in diameter. The imaging protocol included a T2-weighted sequence for volumetric measurement, and the dynamic study using a small molecular weight agent Gd-DTPA-BMA (¤Omniscan, 0.1 mmol/kg), followed by an intermediate molecular weight agent Gadomer-17 (0.05 mmol/kg, provided by Schering AG, Germany). After the MRI study was completed the rats received i.v. injection of 4 mg/kg Taxotere. Three follow-up MRI studies were performed, once per week (noted as W1, W2, and W3). The rats continued to receive weekly Taxotere treatment after each MRI study. The volume of each tumor was measured from the T2-weighted images, and depending on the volumes at W3 compared to the baseline, the tumors were separated into responders (volume decreased by 50%), non-responders (volume increased by 50%), and stabilizer (others). Also, the response at each time point (W1, W2 and W3) compared to the baseline was analyzed separately. The MRI enhancement parameters (at 30 sec, 1-min, and 2-min-approximately the maximum enhancement after contrast injection) and the K21 decay rate were used to investigate whether any of these parameters themselves, or the changes compared to the previous time measures, can be used to differentiate responders from non-responders at a later time.

Results

Among these 35 tumors, 29 tumors (20 IDC, 3 NPC, 4 FA, 1 adenosis, and 1 papilloma) have completed the longitudinal study at 4 time points. According to the tumor volume at the end of week-3 compared to the baseline (noted as GR), the tumor was classified into responder (GR < 0.5), stabilizer (0.5 < GR <1.5), and non-responder (GR > 1.5). Of the 20 IDC, 9 were responders, 5 were stabilizers, and 6 were non-responders. Interestingly all 3 NPC were stabilizer. Three fibroadenomas were non-responders and another FA was a responder. Figure 1 shows the T2-weighted images and the contrast enhancement kinetics measured from an infiltrating adenocarcinoma which showed a consistent regression with treatment. Figure 2 shows another infiltrating adenocarcinoma which apparently did not respond to treatment. The tumor grew larger over the three weeks period. However, not every tumor was responding consistently. Some would grow bigger at week-1, then started to shrink, and some would shrink first and later grew larger. Given the complicated response pattern, the statistical analysis was only performed for IDC and the response at each time point was analyzed separately. Tumor size at week-1 compared to the baseline was calculated, and separated into +/- growth groups. Among all 8 MRI parameters, the baseline Gadomer-17 enhancements at 1-min and 2-min at baseline showed a significant difference ($p < 0.05$, Wilcoxon rank-sum tests) between the 2 groups with +/- growth at week-1. The same analysis was applied at week-2 and week-3, but the tests indicated that no MRI parameters revealed a significant difference between different growth groups at week-2 and week-3.

One responder (infiltrating ductal adenocarcinoma)

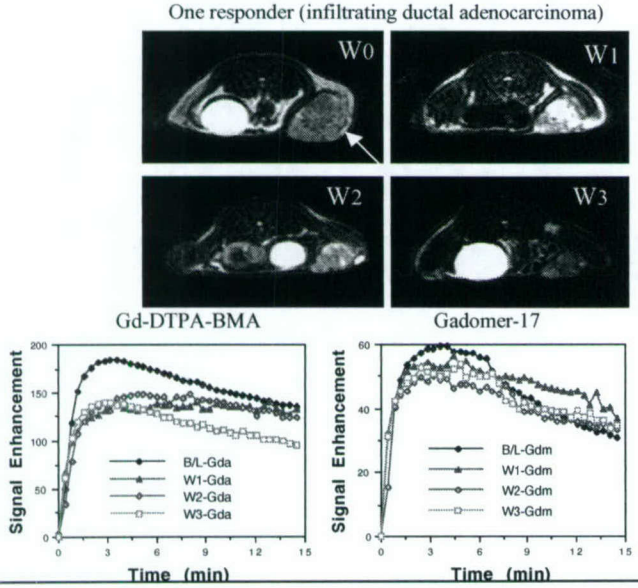

Figure 1: The T2-weighted image, and the enhancement kinetics measured by Gd-DTPA-BMA and Gadomer-17 in one responder tumor (infiltrating ductal adenocarcinoma). The tumor showed continuous regression over time. The kinetics measured by Gd-DTPA-BMA showed reduced intensity after the first treatment, and the pattern of the curve became more flattened (i.e. no wash-out).

One non-responder (infiltrating ductal adenocarcinoma)

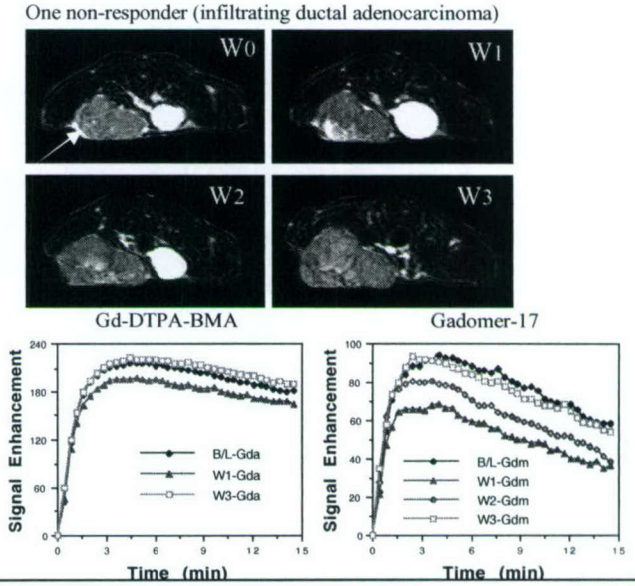

Figure 2: The T2-weighted image, and the enhancement kinetics measured by Gd-DTPA-BMA and Gadomer-17 in one non-responder tumor (infiltrating ductal adenocarcinoma). Apparently the tumor grew larger and larger over time. The Gd-DTPA-BMA kinetics were similar over time, and the Gadomer-17 kinetics showed a great reduction at Week-1 then recovered to the baseline level at Week-3.

Discussion

In this study we investigated the volumetric changes and contrast enhancement changes in ENU induced tumors receiving Taxotere, as measured by longitudinal MRI. The ENU induced benign and malignant tumors, and the malignant came with 2 major types, infiltrating ductal adenocarcinoma, and non-infiltrating papillary adenocarcinoma (simulating in-situ cancers). Among all tests, only the baseline Gadomer-17 enhancements at 1-min and 2-min revealed a significant difference between IDC s which grew bigger at week-1 versus those which shrank at week-1. This maybe interpreted as that tumors with a higher vascularity measured by Gadomer-17 (a blood pool contrast medium) had a better response (showing shrinkage), possibly due to more drug delivery. However, the data also indicated that not only ENU induced tumors came with a large variation, they also showed different responses to therapy. Although ENU induced tumors may simulate the variety in human breast cancer, but it may not be a good tumor model for drug response testing.

Acknowledgement

This work was supported in part by a grant from DOD ARMY BCRP No. DAMD17-01-0178.

Appendix- All Related Publications (8/2001 - 7/2004)

DAMD17-01-1-0178
Anti-Angiogenic Therapeutic Indicators in Breast Cancer
Min-Ying Su, PhD

Journal Paper:

Min-Ying. Su, Hon Yu, Jr-Yuan Chiou, Jun Wang, John P. Fruehauf, Orhan Nalcioglu, Rita S. Mehta, and Choong Hyun Baick. Measurements of Volumetric Changes and Vascular Changes with Dynamic Contrast Enhanced MRI for Cancer Therapy Monitoring. Technology in Cancer Research and Treatment, **1**(6): 479-488, 2002.

M. Samoszuk, L. Leonor, F. Espinoza, P. M . Carpenter, O. Nalcioglu, and M.-Y. Su. Measuring microvascular density in tumors by digital dissection. Analytical and Quantitative Cytology and Histology **24**(1):15-22, 2002.

Conference Abstracts:

M-Y. Su, M. J. Hamamura, H. Wang, H. J. Yu, J. Wang, P. M. Carpenter, O. Nalcioglu. Monitoring Chemotherapy Induced Changes in the Carcinogen ENU Induced Infiltrating Ductal Adenocarcinoma and Non-Infiltrating Papillary Adenocarcinoma by Longitudinal MRI Studies. "Proc., 12th ISMRM Annual Meeting, Kyoto, Japan, 2004" p2373.

Min-Ying Su, Hon Yu, Jun Wang, Phillip Carpenter, John Fruehauf, and Orhan Nalcioglu, "Characterization of Angiogenesis in The Carcinogen ENU Induced Benign And Malignant Mammary Tumor Model". in "Proc., 11th ISMRM Annual Meeting, Toronto, 2003"

Min-Ying Su, Hon Yu, Jun Wang, Orhan Nalcioglu, "Characterization Of Angiogenesis in The Carcinogen ENU Induced Benign And Malignant Mammary Tumor Model" Second Era of Hope meeting (Department of Defense Breast Cancer Research Program Meeting), Orlando, FL, 2002

Min-Ying Su, Michael Samoszuk[2], Leonard Leoner, Phillip M. Carpenter[2], and Orhan Nalcioglu, Quantitative Vascular Density Assessed by a Semiautomatic Histological Method in Comparison with MRI Enhancements in Carcinogen Induced Benign and Malignant Mammary Tumors in Rats. . in "Proc., 10th ISMRM Annual Meeting, Hawaii, 2002" p2108.

Hon Yu, Min-Ying Su, Jun Wang, and Orhan Nalcioglu, Longitudinal Taxotere Chemotherapy Treatment Induced Vascular and Structural Changes Measured by Dynamic Enhanced MRI. in "Proc., 10th ISMRM Annual Meeting, Hawaii, 2002" p2131.

Hon Yu, Min-Ying Su, Jun Wang, Phillip M. Carpenter[2], and Orhan Nalcioglu, Characterization of Carcinogen ENU Induced Benign and Malignant Mammary Tumors in Rats: Volumetric Growth Rates, Contrast Enhancement Kinetics, and Longitudinal Monitoring. in "Proc., 10th ISMRM Annual Meeting, Hawaii, 2002" p2180.

Technology in Cancer Research & Treatment
ISSN 1533-0346
Volume 1, Number 6, December (2002)

Measurement of Volumetric and Vascular Changes with Dynamic Contrast Enhanced MRI for Cancer Therapy Monitoring

www.tcrt.org

Min-Ying. Su, Ph.D.[1,*]
Hon Yu, M.S.[1]
Jr-Yuan Chiou, Ph.D.[1]
Jun Wang, M.D.[1]
Orhan Nalcioglu, Ph.D.[1]
John P. Fruehauf MD Ph.D.[2]
Rita S. Mehta, M.D.[3]
Choong Hyun Baick, M.D.[4]

[1]John Tu & Thomas Yuen Center for Functional Onco-Imaging
University of California
Irvine Hall 164
Irvine, CA 92697-5020, USA
[2]Oncotech Inc. Tustin, CA
[3]Department of Medicine, UC Irvine
[4]Department of Surgery, UC Irvine

Longitudinal dynamic contrast enhanced MRI studies were undertaken to monitor therapy induced volumetric and vascular changes. Three study components are presented in this work: one animal tumor chemotherapy study (R3230 AC adenocarcinoma treated with Taxotere), one patient with invasive lobular breast cancer undergoing neoadjuvant chemotherapy (AC regimen), and one patient with brain metastasis of primary breast cancer undergoing radiation therapy (40 Gray whole brain irradiation). In the animal study two contrast media with different molecular weights, Gadodiamide and Gadomer-17, were used. Only Gadomer-17 revealed significant changes in vascular properties. The responders showed decreased V_b (vascular volume index) and K_2 (out-flux transport rate), which preceded tumor regression. The control tumors showed increased V_b and K_2, before tumor growth became much faster. In the patient undergoing neoadjuvant therapy, the tumor was shrinking by 45% after 2 cycles of treatment, then again by 45% after 2 additional cycles. K_2 was decreasing over time with treatment. In the patient with brain metastasis, the 2 follow-up studies were much longer apart to monitor the regression and relapse of lesions. The pre-treatment volumes of lesions in the group without recurrence were significantly smaller compared to those with recurrence. In summary, the tumor volume was more sensitive than the vascular parameters measured by the small extracellular contrast medium for the assessment of therapy response and prediction of recurrence. The vascular properties measured by macromolecular contrast medium may have the potential to serve as early therapeutic efficacy indicators.

Key words: Contrast Enhanced MRI, Breast cancer, Chemotherapy, Radiation therapy, Therapy response

Introduction

Locally advanced breast cancer may be unresectable due to its invasion. Neoadjuvant chemotherapy may downstage the tumor, decrease the tumor size and render tumor resectable (1-2). Recent trend of breast conservation therapy encourages patients to receive down-staging neoadjuvant chemotherapy, even if cancers are readily operable, to avoid mastectomy or to improve prognosis (3-5). Furthermore, neoadjuvant chemotherapy may be used as an in vivo measure of tumor response to treatment, especially to evaluate the benefits of new treatment approaches (6-9). In parallel it has become increasingly important to develop reliable monitoring methods to measure the response of cancer at early times after the therapy is initiated. If therapy failure can be predicted early, it can be aborted to spare the patient from ineffective treatment and the associated morbidity. MRI provides great soft tissue contrast, and the post enhanced image after administration of contrast medium provides clear tumor margin for its delin-

* Corresponding Author:
Min-Ying Su, Ph.D.
Email: msu@uci.edu

eation, thus may be the best imaging modality for monitoring therapeutic response of breast cancer (10-14). When the enhancement kinetics is acquired dynamically, the vascular properties of the tumor can be obtained by performing pharmacokinetic analysis (15-16). Dynamic contrast enhanced MRI maybe applied longitudinally to reveal therapy induced vascular changes occurring in the tumor. In this study, we investigated whether the changes in the vascular parameters were associated with the final therapeutic response, thus might serve as early therapeutic indicators.

Three study components are included in this work. We first used an animal model (R3230 AC adenocarcinoma treated with Taxotere) for the development of study protocol and analysis methods. Pixel-by-pixel analysis was performed to handle the tumor heterogeneity problem (17). The pixel population distribution curves of vascular volume index (V_b) and vascular permeability index (out-flux transport rate K_2) were calculated. The longitudinal vascular changes were measured to determine whether they precede the volumetric changes of tumors, thus may serve as therapeutic indicators. In the animal study, we used two different contrast media, Gadodiamide (<1 kD) and Gadomer-17 (35 kD). It is known that the macromolecular contrast medium (MMCM) may reveal the vascular properties more accurately (18-19). The results obtained from the two contrast media were compared.

The same study protocol and the analysis methods were applied to two human studies: a patient with breast cancer receiving neoadjuvant chemotherapy (AC regimen), and a patient with metastatic breast cancer in the brain receiving radiation therapy. A pre-treatment and two follow-up studies were performed for each patient. In the breast cancer neoadjuvant therapy study, the volumetric changes and the vascular changes (V_b and K_2) occurring in the lesion after completing 2 cycles and 4 cycles of treatment were compared to investigate their relationship. In the brain metastasis radiation therapy study, the two follow-up studies were performed to measure remission and then relapse of lesions. The volume and the vascular properties of lesions in the baseline study were analyzed with respect to their recurrence status to investigate whether they can predict the recurrence.

Materials and Methods

Animal Tumor Chemotherapy Study

Nine female Fischer-344 rats (160 ~ 170 g) bearing the R3230 AC adenocarcinomas were used in the study. A small fragment of tumor harvested from a donor rat was implanted subcutaneously into a rat. When the tumor grew to 0.8 cm in diameter (approximately 3 weeks after implantation), the baseline MRI study was conducted. The animal MRI experiments were performed on a 3.0-T scanner using a Marconi console (Cleveland, OH). One set of T2-weighted images covering across the tumor were acquired for volumetric measurements, using a fast spin echo sequence with TR=5500ms, TE=105.6 ms and 8 echo train. Then a T1-weighted sequence (RF-FAST VOL, with TR/TE = 18/3.6 ms and flip angle=20°) was used for the dynamic contrast enhancement study. A total of 40 acquisitions were prescribed. The temporal resolution was 24 sec for each acquisition. The contrast medium was injected as a short bolus after the first 4 acquisitions have been completed. In this animal study, two contrast media, an extracellular agent Gadodiamide (0.1 mmol Gd/kg Omniscan®, Nycomed Inc. Princeton, NJ) and a medium-sized agent Gadomer-17 (0.05 mmol Gd/kg), were injected sequentially. Gadomer-17 was a dendrimeric compound with size equivalent to a 35 kD protein, provided by Schering AG (Berlin, Germany). Firstly, Gadodiamide was injected and the enhancement kinetics were measured. After waiting 1 hour for the clearance of Gadodiamide, Gadomer-17 was injected and the enhancement kinetics were measured. After the baseline MRI was completed, six of the nine rats received i.v. injection of Taxotere (4 mg/kg, Aventis Pharmaceuticals Products Inc. Collegeville, PA) for chemotherapy. All rats were scanned at one week (week-1), two weeks (week-2) and three weeks (week-3) after the baseline study (week-0) for follow-up. The same imaging protocol with 2 sequentially injected contrast medium was used in all studies. The rats in the treated group received chemotherapy weekly, after each MRI study.

The total tumor volume was measured by manually outlining the tumor region on T2-weighted images. The viable tumor volume (determined as the enhanced tumor regions) was measured by threshold segmentation based on Gadodiamide enhanced images. The detailed procedure has been published previously (17). Figure 1a shows the growth curve of viable tumor volumes in 6 rats. It can be seen that the largest difference between controls and treated tumors happened at week-3. The ratio of week-3 volume divided by week-2 volume was used to categorize the degree of responses, as shown in Figure 1b. Those tumors shrinking between week-2 and week-3 were categorized as responders, and those still growing but at a slower rate compared to the controls were categorized as partial responders (not shown in Fig. 1a). Three of the six treated rats were classified as responders (with week-3/week-2 growth ratios of 0.82, 0.88 and 0.88), whereas the other three treated rats were classified as partial responders as their ratios were greater than 1 (1.07, 1.22 and 1.26), but still lower than the control group's ratios (1.92, 1.93 and 2.24). Since the most volumetric group differences happened between week-2 and week-3, we were interested in measuring changes in the enhancement kinetics prior to the changes in tumor volume occurred, i.e. between week-1 and week-2. In addition to the overall enhancement kinetics, the changes in the pixel population distribution curves of

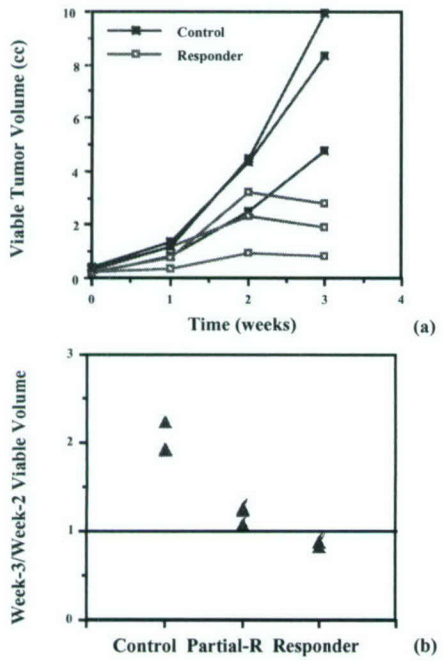

Figure 1: The growth curve of the viable tumor volume in 3 control and 3 responder rats. The most difference happened at wek-3. The ratio between week-3 and week-2 viable tumor volume was used to separate responders (ratio <1: 0.82, 0.88, 0.88) and partial responders (ratio >1: 1.07, 1.22, 1.26) from controls (1.92, 1.93, 2.24).

pharmacokinetic parameters were measured. All pixels contained within the viable region of each tumor were analyzed on a pixel-by-pixel basis by using a 2-compartmental pharmacokinetic model, as described next.

Pharmacokinetic Analysis and Pixel Population Distribution

A 2-compartmental model can be used to describe the transport of contrast medium in tissue vascular and interstitial spaces as a function of time, which allows the determination of the relative tracer concentration in these two tissue compartments. The details of the methodology have been described in previous publications (20-21). Briefly, the transport of tracer from the plasma compartment into the extravascular compartment can be expressed as Eq. [1].

$$V_e \frac{dC_e}{dt} = k_1 C_p - k_2 C_e \qquad 1(a)$$

$$\text{or} \quad \frac{dC_e}{dt} = K_1 C_p - K_2 C_e \qquad 1(b))$$

where K_1 and K_2 are defined as $K_1 \equiv k_1 / V_e$, and $K_2 \equiv k_2 / V_e$. C_p and C_e are the tracer concentrations in the plasma and extravascular compartments, V_e is the distribution volume of the contrast medium in the extravascular extracellular space, k_1 is the in-flux transport rate from plasma to interstitial space, and k_2 is the out-flux transport rate from interstitial space back into plasma. K_1 and K_2 are the transport constants related to the leakage space, whereas k_1 and k_2 are related to whole tissue. Total enhancement kinetics constituted the contributions from both the vascular and the extravascular compartments. The total concentration in a selected region of interest in tissue, C_T, is from the contributions of both plasma and extravascular compartments, as shown in Eq. [2].

$$C_T(t) = V_p \cdot C_p(t) + V_e \cdot C_e(t) = V_b \cdot C_b(t) + V_e \cdot C_e(t) \qquad [2]$$

where C_P is the contrast medium concentration in plasma, which is related to (Gd) in blood by $C_b = C_p(1\text{-Hct})$, Hct = hematocrit, V_p is the plasma volume fraction (blood volume $V_b = V_p/(1\text{-Hct})$), and V_e is the leakage space fraction in the selected ROI.

A Non-Linear Least squares (NLLS) fitting was applied to analyze the measured enhancement kinetic curve, for obtaining three independent fitting parameters from the best fit. These three parameters were: the apparent vascular volume (V_b), the product of the in-flux transport rate and the distribution volume in the interstitial space (V_eK_1), and the out-flux transport rate (K_2). The analysis process was similar to that described by Tofts, who proposed a unified model that reconciles various models proposed by different research groups (15). Our notation V_eK_1 is equivalent to ($kin^{PS\rho}$), and K_2 is equivalent to ($kout^{PS\rho}/V_e$) used in the unified model.

The enhancement kinetics from each pixel was measured then fitted with the pharmacokinetic model to obtain the vascular volume (V_b) and the out-flux transport rate (K_2). For each parameter, the values from all pixels of 3 tumors in each study group were pooled together and sorted in a descending order, then the cut-off values of the top 90% pixels, 80% pixels, 10% pixels were determined to generate the pixel population distribution curve. The detailed procedure has been published previously (17).

Monitoring Neoadjuvant Chemotherapy in A Patient with Breast Cancer

The similar study protocol and analysis methods used for the animal study were used for the human study. Dynamic contrast enhanced MRI was applied to monitor the efficacy of neoadjuvant chemotherapy in a 48-year-old women with invasive lobular breast cancer. The MRI scan was performed on a 1.5 Tesla Marconi Eclipse system (Cleveland, OH) with a dedicated breast coil. The dynamic acquisition was performed using a 3D gradient echo pulse sequence (RF-FAST VOL) with TR/TE = 10/3.6 ms, flip angle = 20°, and acquisition

matrix = 256×128. The temporal resolution was 42 sec for one acquisition. The FOV (Field of view) was 32 cm. Thirty-two slices with 4 mm thickness were used to cover both breasts. Sixteen frames were prescribed. The contrast medium Gadodiamide (1cc Omniscan® per 10 lbs body weight, Nycomed Inc. Princeton, NJ) was injected after 4 acquisitions were completed. The post contrast images were acquired for the next 12 frames, lasting approximately 8 minutes after injection. After the baseline MRI, the patient received AC regimen chemotherapy (Adrimycine and Cyclophosphamide). The follow-up MRI exam was performed at 2 weeks after completing 2 cycles, then again at 2 weeks after completing 4 cycles to measure the therapy induced changes.

The analysis was similar to that used in animal studies. The tumor regions were determined from contrast enhancement maps. The color-coded enhancement maps were obtained by subtracting the mean pre-contrast image (averaged over the first 4 frames) from the 2-min post enhanced image (the 8th frame). The color-coding scale was fixed in the analysis of all 3 MRI studies, so that the tumor regions could be determined with a consistent criterion. The enhancement maps of one slice containing a tumor mass in the 3 MRI studies are shown in Figure 2a. It clearly demonstrated that the tumor was shrinking. A boundary covering the entire bilateral breast region was drawn for the pixel-by-pixel analysis. The enhancement kinetics of all pixels contained within this boundary were measured, then analyzed with the pharmacokinetic model to obtain the parameters. These fitted parameters were then used to construct the pharmacokinetic maps, shown in Figure 2b for V_b and Figure 2c for K_2. The fitting parameters obtained from all tumor pixels were separately obtained to calculate the pixel population distribution curves. The V_b and K_2 curves in the pre-treatment and the 2 post-treatment studies were compared.

Assessment of Recurrence in A Patient with Metastatic Breast Cancer in the Brain

The similar study protocol was applied to study one female patient (54-year-old) with metastatic breast cancer in the brain. A baseline MRI was performed before initiation of radiation therapy. Then the patient received 40 Gray whole brain radiation therapy for 4 weeks. A follow-up MRI was performed at 2 months after the radiation therapy was completed. Almost all metastatic lesions in the first follow-up study disappeared, thus the changes in the enhancement kinetics were not assessed. Then 6 months later the third MRI was performed to examine the recurrence of brain metastasis. Therefore, in this study instead of investigating the therapy induced short-term changes, we were interested in studying the indicators for recurrence. The dynamic contrast enhanced MRI was acquired using the same 3D gradient echo pulse sequence (RF-FAST VOL). The parameters were: coronal view, TR = 10 ms, TE = 3.63 ms, flip angle = 20 degree, slice thickness = 6 mm, FOV = 22 cm, image matrix = 256×128×28, number of frames = 16. The temporal resolution for each acquisition was 34 sec. Since many small lesions were identified, image registration was required to locate the corresponding lesions in different studies. The realignment program provided in SPM99 (Statistical Parametric Mapping, Developed by members & collaborators of the Wellcome Department of Cognitive Neurology, UK) was used to register the set of 3D images taken in the follow-up studies to those in the baseline study. Figure 3a shows the realigned contrast enhanced images from 4 consecutive slices (columns) acquired in 3 studies (rows). As noted in the figure, 7 lesions were identified from these 4 slices in the baseline study. Most lesions disappeared or became very small with a much lower contrast enhancement at the 3-month follow-up study (2 months after completing radiation therapy). Six months later in the second follow-up study, some lesions did not recur, some recurred but with a small size, and some lesions were with a large size, even bigger than their initial size in the baseline study.

Table I

The volumes of 7 lesions in the baseline and the 2nd follow-up studies in Figure 3

Lesions	Baseline volume (cc)	2nd follow-up volume (cc)
1	0.45	0.44
2	0.96	0.08
3	1.20	1.18
4	0.26	0
5	0.50	0
6	0.97	0
7	1.28	0.07

The color-coded enhancement maps were obtained, and from which the tumor region was outlined to measure the volume of each lesion. Figure 3b shows the corresponding enhancement maps of the 4 slices. The darker reddish color represents a higher enhancement. Only lesions exhibiting red enhancement color was counted. Some larger lesions were found to extend into the neighboring slices. By carefully examining their relative locations, we could identify whether a lesion shown on one slice was a separate lesion or was a part of a lesion from the previous slice. All together, 32 lesions were identified in the baseline study. The volumes of the 7 identified lesions shown in Figure 3 in the baseline and the second follow-up studies are listed in Table I. Lesions 4, 5 and 6 did not recur. Lesions 2 and 7 recurred but with a much smaller volume. Lesions 1 and 3 recurred to their baseline sizes. In addition to the volume, the enhancement kinetics of all lesions were analyzed using the same pharmacokinetic analysis methods. For each lesion, the enhancement kinetics of all pixels were measured, then analyzed with the pharmacokinetic model to calculate the pixel population distribution curves of V_b and K_2. We were interested in investigating which baseline characteristics of the lesion (volume,

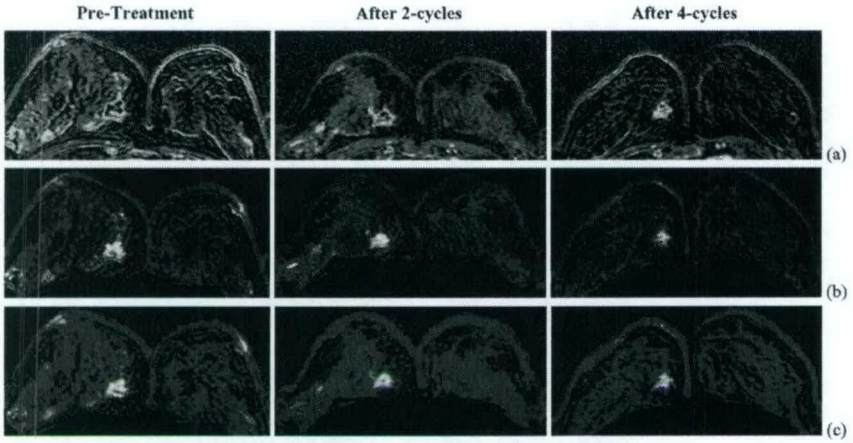

Figure 2: The color-coded enhancement maps (a) of one imaging slice containing a tumor mass in the pre-treatment study and the 2 follow-up studies after completing 2 cycles and 4 cycles treatment. The darker reddish color represents a higher enhancement. The color-coding scale was identical in the 3 MRI studies. The tumor was shrinking with treatment. Pixel-by-pixel pharmacokinetic analysis was performed to obtain the reconstructed V_b (b) and K_2 (c) maps.

V_b and K_2 profile) were associated with the recurrence, thus may be used to predict the recurrence status.

Results

Animal Tumor Chemotherapy Study

The tumor bearing animals tolerated the Taxotere chemotherapy well. However, the therapy did not cause a substantial effect on the R3230 AC adenocarcinoma resulting in shrinkage. The treated tumors showed a slower growth rate compared to the controls. The most difference between control and treated tumors occurred between week-2 and week-3, thus it was used to separate responders and partial responders from controls. The changes in the tumor enhancement kinetics between week-1 and week-2 (before the volumetric change occurred) were studied. Figure 4 shows the pixel population distribution curve of V_b for the control group (Fig. 4a) and the responder group (Fig. 4b) measured with Gadomer-17 at

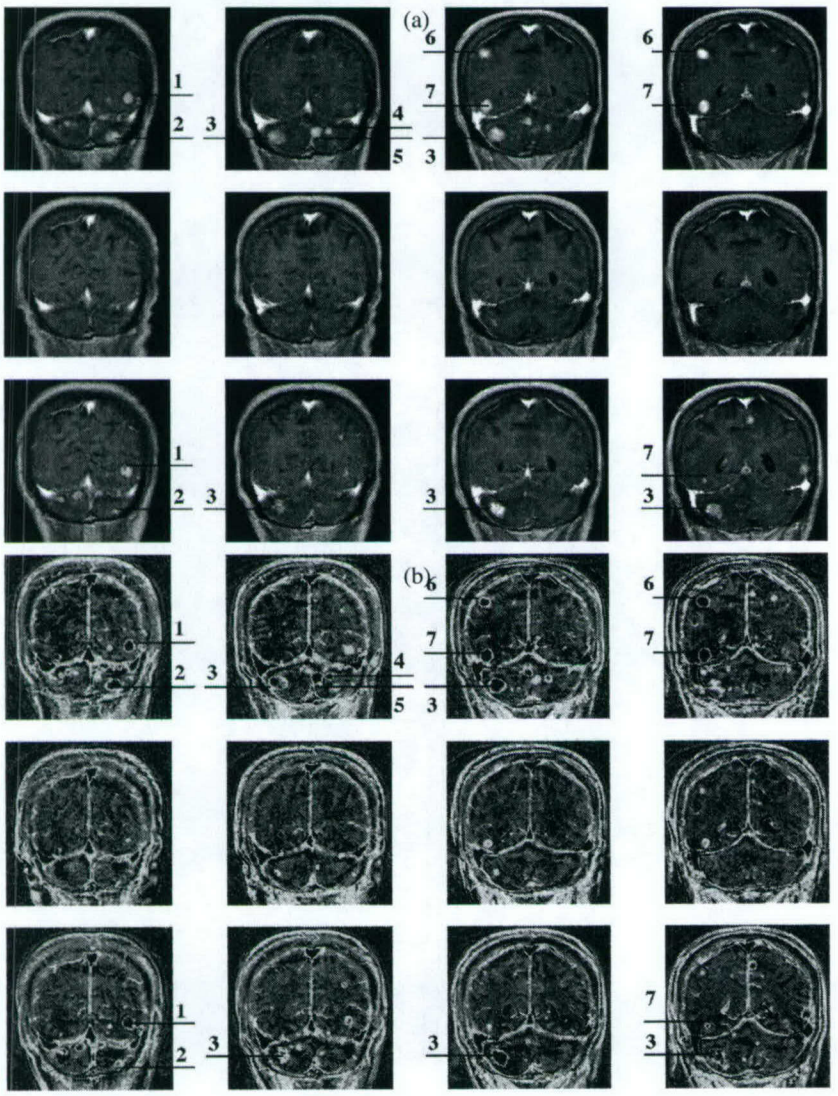

Figure 3: The contrast enhanced images (a) and the color-coded enhancement maps (b) of 4 consecutive imaging slices in the baseline study before treatment (1st row), the first follow-up study when the lesions regressed (2nd row), and the second follow-up study when the lesions relapsed (3rd row). For some large lesions extending into the neighboring slices, they could be identified by the relative location. The volumes of each lesion in the baseline and the second follow-up studies were measured from the color-coded enhancement maps.

week-1 and week-2. In the control group the V_b curve at week-2 was increased throughout the whole population compared to the curve at week-1 (significant from 10^{th} to 70^{th} percentile); whereas in the responder group the distribution at week-2 was reduced with respect to its week-1's curve throughout the whole population (significant from 30^{th} to 70^{th} percentile). Figures 5a and 5b show the pixel population distribution curves of K_2 at week-1 and week-2 measured with Gadomer-17 for the control and responder groups, respectively. In the control group the K_2 was increased throughout the population (significant from 20^{th} to 80^{th} percentile). Interestingly that was associated with the much faster growth of tumors subsequently from week-2 to week-3. In contrast the responders showed decreased K_2, but it was not statistically significant. The changes in the V_b and K_2 profiles from week-1 to week-2 were opposite between controls and responders. The partial responder group showed an increased V_b at week-2 with respect to week-1's and showed a decreased K_2. Similar procedures were performed to analyze the enhancement kinetics measured by the smaller extracellular agent Gadodiamide. The V_b and K_2 distribution curves did not show any significant changes among these 3 groups.

Monitoring Neoadjuvant Chemotherapy in A Patient with Breast Cancer

In the breast patient study only the clinically approved small contrast medium Gadodiamide was used. Three MRI studies were performed, one pre-treatment and 2 follow-up's at 2 weeks after 2 cycles of treatment and 2 weeks after 4 cycles of treatment. The biopsy results showed that the patient had confirmed multi-focal lobular cancers at 2 different sites. The image slice shown in Figure 2 only covered one mass at one site. The volumes of this mass were 3.7 cc at baseline, 2.0 cc after 2-cycles of treatment and 1.1 cc after 4-cycles of treatment. The tumor shrank by 45% after 2-cycles, then again shrank by 45% after 2 more cycles. The other mass connecting to this one, and the tumor at another site all

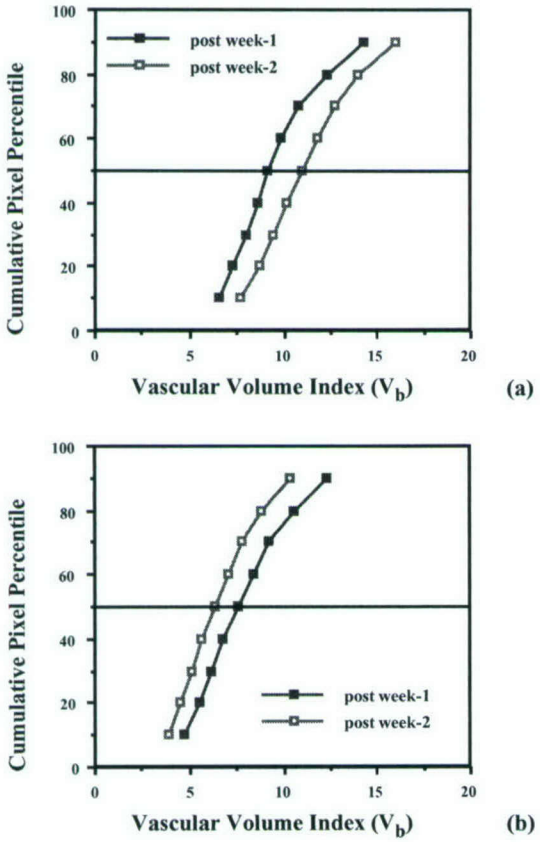

Figure 4: The pixel population distribution curves of the vascular volume index (V_b) in the control (a) and the responder (b) groups at week-1 and week-2. In the control group, the V_b shifted to higher values at week-2 throughout the entire population; whereas in the responder group the V_b was reduced at week-2 compared to week-1.

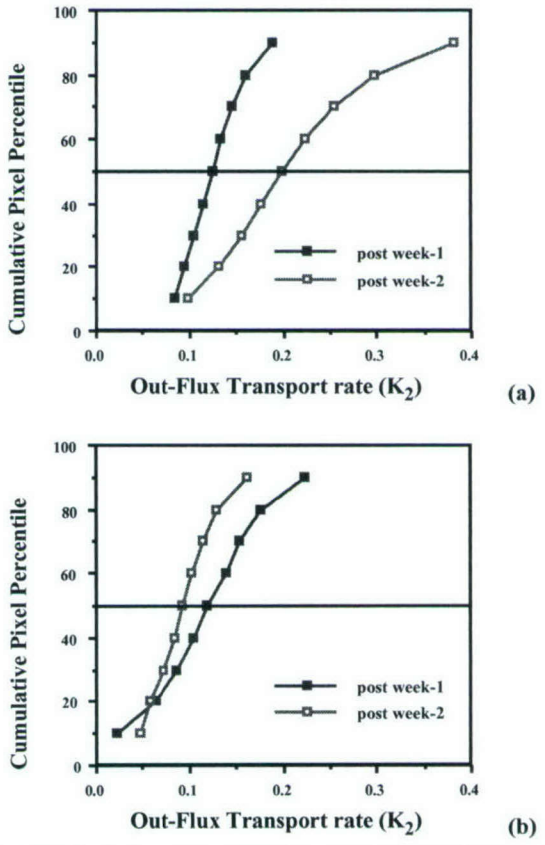

Figure 5: The pixel population distribution curves of the out-flux transport rate (K_2) in the control (a) and the responder (b) groups at week-1 and week-2. In the control group, the K_2 was increased at week-2 throughout the entire population. Interestingly that was associated with the much faster growth rate subsequently between week-2 and week-3 (shown in Fig. 1a). In the responder group the K_2 was reduced at week-2 compared to week-1.

showed similar responses and a comparable shrinkage rate. Figure 6a shows the enhancement kinetics measured from this mass at the 3 time points, using the region of interest analysis covering the entire mass. The baseline kinetics had the highest magnitude and a clear wash-out phase. The magnitude of enhancement decreased with treatment. All pixels contained within this mass were analyzed on a pixel-by-pixel basis, then the V_b and K_2 population distribution curves were calculated. The V_b and K_2 curves in the 3 MRI studies are shown in Figure 6b and 6c, respectively. In the V_b distribution profile, the pre-treatment and the post 2-cycles studies had similar curves, and the post 4-cycles study had substantially lower V_b values. In the K_2 distribution profile, it demonstrated a reduced K_2 over time with treatment. For all analyzed parameters, the tumor volume was the one showing the highest percentage change with treatment.

Assessment of Recurrence in A Patient with Metastatic Breast Cancer in the Brain

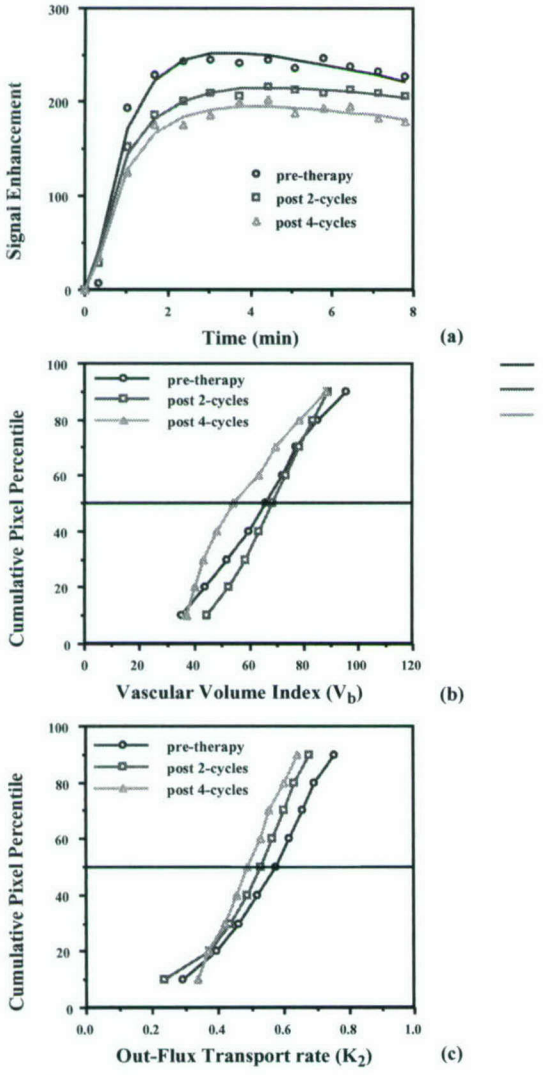

Figure 6: The contrast enhancement kinetics (a) measured from the mass shown in Figure 2 at three time points. The lesion exhibited a slower upslope and lower enhancement magnitude after receiving treatment. The wash-out rate became flattened after treatment. Pixel-by-pixel analysis was performed to obtain the population distribution curve of V_b (c) and K_2 (c) in all 3 MRI studies. The V_b was reduced at post 4-cycles, and the K_2 was decreasing with treatment.

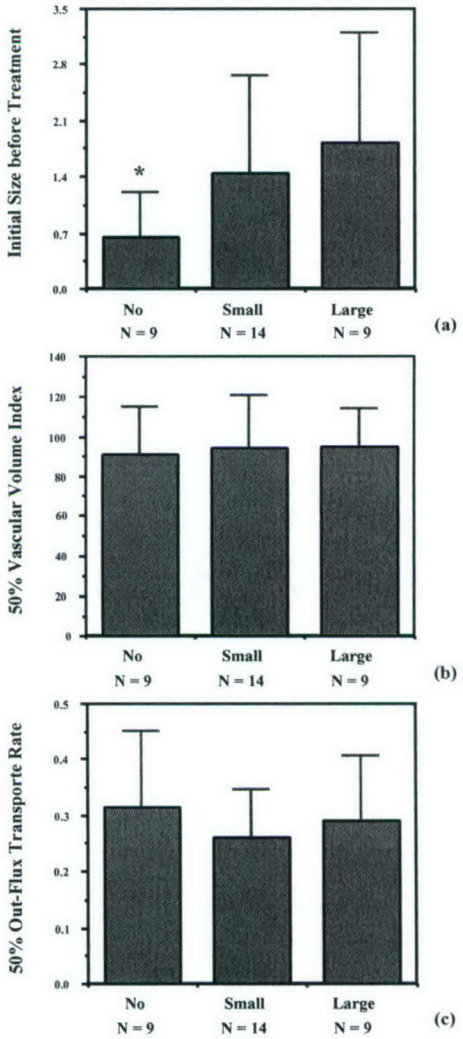

Figure 7: Thirty-two brain metastatic lesions identified in the baseline study were separated into three groups according to their recurrence size (no recurrence, volume < 0.45, or volume > 0.48) in the second follow-up study. The baseline volume (a) and the median V_b (b) and median K_2 (c) of lesions in each group are shown. The error bar represents the standard deviation. Only the baseline volume was associated with the recurrence status (significantly lower in the no-recurrence group).

In this brain metastasis study similarly three MRI studies were performed, one before radiation therapy, and 2 follow-up's at 2 months and 8 months after completing a treatment regimen of 4-weeks-long 40 Gray whole brain irradiation. By carefully examining the relative location of all lesions shown on contrast enhanced images, 32 separate lesions were identified in the baseline study. In the first follow-up study, these lesions either totally disappeared or became very small and showed a much lower enhancement. In the second follow-up study, some lesions recurred, some did not, and also some new lesions appeared. By co-registering all images in the 3 studies, we were able to match the lesion locations to determine the recurrence size of each of the 32 lesion. Nine lesions did not recur; 14 lesions recurred with a volume less than 0.45 cc; and 9 lesions recurred with a volume greater than 0.48 cc. The largest recurrence lesion size was 4.0 cc. According to their recurrence size, the 32 baseline lesions were separated into 3 groups. The baseline volume and the enhancement kinetics of all lesions in each group were measured then compared between groups. Figure 7a shows the baseline volumes of lesions in these 3 groups. The group without recurrence had a significantly smaller volume (0.65 ± 0.55 cc) than the group with small recurrence (1.45 ± 1.20 cc) or the group with large recurrence (1.83 ± 1.37 cc). The difference between the later 2 groups was not significant. The enhancement kinetics of all pixels contained within each lesion were measured then analyzed with the pharmacokinetic model to obtain the V_b and K_2 population distribution curves. The median V_b and K_2 of each lesion was obtained for statistical analysis. Figures 7b and 7c show the mean value of the median V_b and K_2 for the 3 groups, respectively. Apparently there was no difference in the baseline median V_b or median K_2 of lesions in these 3 groups. Similar analysis was performed for all pixel percentile values (10^{th} to 90^{th}). None of these V_b or K_2 values showed significant differences among the three groups.

Discussion

We reported three studies in this work, an animal tumor chemotherapy study, a human breast cancer neoadjuvant chemotherapy study, and a human metastatic breast cancer radiation study. The similar study protocol and analysis methods were used in all 3 studies. The only difference was that in the animal study we could use a medium-sized macromolecular agent Gadomer-17. This agent is not an FDA approved agent for human study. Pre-treatment and follow-up studies were performed to measure the changes of tumor volumes and the vascular properties over time. In the first 2 chemotherapy studies, the relationship between volumetric changes and vascular changes were investigated. If earlier vascular changes were associated with subsequent volumetric changes, then they may serve as early therapeutic indicators to predict final outcome. The nature of the radiation therapy study was different from the 2 chemotherapy studies. The follow-up times were longer to study remission (1^{st} follow-up, 2 months after completing radiation therapy) then relapse (2^{nd} follow-up, 6 months after the 1^{st} follow-up) of brain metastasis. We investigated whether the baseline lesion volume or the vascular properties were associated with the recurrence status. If such relationships can be found, one may predict which lesion is more likely to recur.

In the animal studies the tumors were separated into responders and partial-responders according to their volumetric growth curves (Fig. 1). Since the largest volumetric differences happened between week-2 and week-3, the changes of vascular properties between week-1 and week-2 were of interest. The vascular volume index (V_b) and the permeability index (K_2) measured by Gadomer-17 showed significant changes between controls and responders. In the control group, the V_b and the K_2 (Figs. 4a and 5a) increased from week-1 to week-2, which was associated with the much faster growth rate between week-2 and week-3 (Fig. 1a). In the responder group the V_b and K_2 decreased (Figs. 4b and 5b), which was associated with the subsequent regression between week-2 and week-3 (Fig. 1a). In the partial responder group the V_b increased from week-1 to week-2 but the K_2 decreased. The partial responder tumors still grew between week-2 and week-3 but at a much slower rate compared to control tumors. The results suggest that the early vascular changes in V_b and K_2 as measured by a macromolecular contrast agent such as Gadomer-17 could possibly serve to predict the treatment efficacy. Similar analysis was performed to analyze the vascular properties measured by the small extracellular agent Gadodiamide. But not any significant changes were observed between groups. The results were consistent with the findings reported in an earlier publication studying R3230 AC tumor receiving Mitomycinc-C chemotherapy (17). The utility of macromolecular contrast medium (MMCM)-enhanced MRI for tumor angiogenesis characterizations has been established experimentally in a range of cancer types including breast, ovary, fibrosarcoma, and prostate (22).

In the human breast cancer neoadjuvant chemotherapy, the volumetric shrinkage was the most pronounced feature among all parameters analyzed. The lesion shown in Figure 2 showed a 45 % reduction in size for every 2 cycles of treatment. The enhancement kinetics measured from the remaining lesion showed a slower up-slope, a lower enhancement magnitude, and a flattened wash-out phase after treatment (Fig. 5a). The enhancement kinetics was greatly dependent on the region of interest covering the lesion. In our analysis the tumor region was outlined based on color-coded enhancement maps obtained at 2-min post contrast injection (Fig. 2b). A consistent color-coding scale was used in all 3 MRI studies. Only regions showing a red color coding were included in the tumor ROI. Therefore, it was not surprisingly that the

enhancement kinetics did not show substantial changes. If the tumor ROI in the follow-up studies enclosed a larger region with lower enhancements, then the volumetric shrinkage rate would be smaller, and the changes in the enhancement kinetics would be greater. In the pharmacokinetic analysis, a reduced V_b in the second follow-up study (Fig. 5b), and a trend of decreasing K_2 over time with treatment (Fig. 5c) were observed. The percentage changes in V_b and K_2 were much smaller than the percentage change in tumor volume. Since only one case study was presented, significance of this result could not be determined. The same protocol will have to be applied to study a cohort of patients, then the appropriate statistical analysis can be performed to assess the potential of using vascular properties to predict final therapy outcome.

Several studies employing contrast enhanced MRI for monitoring neoadjuvant chemotherapy in breast cancer have been reported. Gilles *et al.* studied 18 patients and showed that early enhancement correlated well with pathological residual tumor (10). Abraham *et al.* applied RODEO MRI technique to determine tumor response and the extent of residual disease in 39 patients, and concluded that MRI performed better than traditional methods of physical exam or mammogram in assessment of response (12). Trecate *et al.* used dynamic contrast enhanced MRI to exam 30 patients, and reported an overall accuracy of 90% (13). Rieber *et al.* reported a series of 58 patients (14). Tumor size and the dynamic contrast medium uptake pattern were evaluated and compared with the final histological findings. The diagnostic accuracy for assigning patients to the non-response (NR) group was 83.3 % and to the partial response (PR) group was 82.4%, but the determination of residual tumor size was unreliable in the complete response (CR) group. Esserman *et al.* investigated the association between MRI phenotype of breast lesions and response to neoadjuvant chemotherapy (23). The circumscribed mass is more likely to respond to therapy (77%) than the other patterns (20-37.5%). No reports are available yet investigating early therapeutic indicators in breast cancer receiving neoadjuvant chemotherapy. In patients with bone or soft-tissue sarcomas, it has been demonstrated that the extent of tumor necrosis and viability measured by dynamic MRI may serve as early predictors for the efficacy (24-25).

In the radiation therapy study the baseline lesion characteristics, including volume and vascular properties, were analyzed with respect to the recurrence status. Similarly, the first step was to determine the tumor region. The color-coded enhancement maps provided a consistent reference for the ROI outlining. The baseline lesion volume was the only parameter showing a significant difference between lesions with and without recurrence. Hawighorst *et al.* reported a study using serial MRI to assess the response of brain metastasis of different primaries receiving radiosurgery and concluded that MRI is a sensitive imaging tool to evaluate tumor response (26). In another study, they used longitudinal pharmacokinetic MRI to monitor the response of malignant brain glioma to stereotactic radiotherapy (27). It was found that a low enhancement amplitude before therapy, combined with an early drop of K_{21} after therapy, can reliably predict subsequent tumor shrinkage. More studies are needed to define the role of longitudinal dynamic contrast enhanced MRI in assessment or prediction of the response of brain metastasis to radiotherapy.

Summarizing from all three studies reported in this work, the changes in tumor size seemed to be the most sensitive response to treatment and to predict recurrence. Contrast enhanced images are definitely required for the tumor volumetric delineation, but the pharmacokinetic vascular properties analyzed from dynamic contrast enhancement studies did not seem to provide additional useful information for monitoring therapy efficacy in human studies. This may due to the use of smaller molecular weight contrast agent (Gadodiamide), that extravasates rapidly into the interstitial space. When the macromolecular contrast media are approved for clinical use, they may provide useful early indicators which are associated with the final therapeutic outcome, as demonstrated in our animal study.

In this study the pharmacokinetic analysis was performed on a pixel-by-pixel basis to handle the problem of tumor heterogeneity. The pixel population distribution curve allows the analysis in the entire population spectrum or in a certain subgroup of pixels. Whether the subpixel population analysis can provide useful information to predict therapy outcome will have to be determined in a study involving larger number of patients.

Acknowledgement

The authors thank Schering AG and Dr. H.-J. Weinmann for providing the medium-sized contrast medium, Gadomer-17. This study was supported in part by the DOD ARMY BCRP grant# DAMD17-01-1-0178, NIH R01 CA90437, and an Avon Breast Cancer Foundation grant funded through the Chao Comprehensive Cancer Center, University of California-Irvine.

References

1. Gianni, L., Valagussa, P., Zambetti, M., Moliterni, A., Capri, G., Bonadonna, G. Adjuvant and neoadjuvant treatment of breast cancer. *Semin. Oncol. 28*, 13-29 (2001).
2. Cance, W. G., Carey, L. A., Calvo, B. F., Sartor, C., Sawyer, L., Moore, D. T., Rosenman, J., Ollila, D. W., Graham, M. Long-term outcome of neoadjuvant therapy for locally advanced breast carcinoma: Effective clinical downstaging allows breast preservation and predicts outstanding local control and survival. *Ann. Surg. 236*, 295-303 (2002).
3. Bonadonna, G., Valagussa, P., Brambilla, C., Ferrari, L., Moliterni, A., Terenziani, M., Zambetti, M. Primary chemotherapy in operable breast cancer: Eight-year experience at the Milan Cancer Institute. *J. Clin. Oncol. 16*, 93-100 (1998).

4. Wolff, A. C., Davidson, N. E. Early operable breast cancer. *Curr. Treat. Options. Oncol. 1*, 210-220 (2000).
5. Wolff, A. C., Davidson, N. E. Preoperative therapy in breast cancer: Lessons from the treatment of locally advanced disease. *Oncologist 7*, 239-245 (2002).
6. Sapunar, F., Smith, I. E. Neoadjuvant chemotherapy for breast cancer. *Ann. Med. 32*, 43-50 (2000).
7. Stebbing, J. J., Gaya, A. The evidence-based use of induction chemotherapy in breast cancer. *Breast Cancer 8*, 23-37 (2001).
8. Aapro, M. S. Neoadjuvant therapy in breast cancer: Can we define its role? *Oncologist Suppl 3*, 36-39 (2001).
9. Smith, I. E., Lipton, L. Preoperative/neoadjuvant medical therapy for early breast cancer. *Lancet Oncol. 2*, 561-570 (2001).
10. Gilles, R., Guinebretiere, J. M., Toussaint, C., Spielman, M., Rietjens, M., Petit, J. Y., Contesso, G., Masselot, J., Vanel, D. Locally advanced breast cancer: Contrast-enhanced subtraction MR imaging of response to preoperative chemotherapy. *Radiology 191*, 633-638 (1994).
11 Knopp, M. V., Brix, G., Junkermann, H. J., Sinn, H. P. MR mammography with pharmacokinetic mapping for monitoring of breast cancer treatment during neoadjuvant therapy. *Magn. Reson. Imaging Clin. N. Am. 2*, 633-658 (1994).
12. Abraham, D. C., Jones, R. C., Jones, S. E., Cheek, J. H., Peters, G. N., Knox, S. M., Grant, M. D., Hampe, D. W., Savino, D. A., Harms, S. E. Evaluation of neoadjuvant chemotherapeutic response of locally advanced breast cancer by magnetic resonance imaging. *Cancer 78*, 91-100 (1996).
13. Trecate, G., Ceglia, E., Stabile, F., Tesoro-Tess, J. D., Mariani, G., Zambetti, M., Musumeci, R. Locally advanced breast cancer treated with primary chemotherapy: Comparison between magnetic resonance imaging and pathologic evaluation of residual disease. *Tumori 85*, 220-228 (1999).
14. Rieber, A., Brambs, H. J., Gabelmann, A., Heilmann, V., Kreienberg, R., Kuhn, T. Breast MRI for monitoring response of primary breast cancer to neo-adjuvant chemotherapy. *Eur. Radiol. 12*, 1711-1719 (2002).
15. Tofts, P. S. Modeling tracer kinetics in dynamic Gd-DTPA MR imaging. *J. Magn. Reson. Imaging. 7*, 91-101 (1997).
16. Tofts, P. S., Brix, G., Buckley, D. L., Evelhoch, J. L., Henderson, E., Knopp, M. V., Larsson, H. B., Lee, T. Y., Mayr, N. A., Parker, G. J., Port, R. E., Taylor, J., Weisskoff, R. M. Estimating kinetic parameters from dynamic contrast-enhanced T(1)-weighted MRI of a diffusable tracer: Standardized quantities and symbols. *J. Magn. Reson. Imaging. 10*, 223-232 (1999).
17. Su, M. Y., Wang, Z., Nalcioglu, O. Investigation of longitudinal vascular changes in control and chemotherapy-treated tumors to serve as therapeutic efficacy predictors. *J. Magn. Reson. Imaging. 9*, 128-137 (1999).
18. van Dijke, C. F., Brasch, R. C., Roberts, T. P., Weidner, N., Mathur, A., Shames, D. M., Mann, J. S., Demsar, F., Lang, P., Schwickert, H. C. Mammary carcinoma model: Correlation of macromolecular contrast-enhanced MR imaging characterizations of tumor microvasculature and histologic capillary density. *Radiology 198*, 813-818 (1996).
19. Daldrup, H., Shames, D. M., Wendland, M., Okuhata, Y., Link, T. M., Rosenau, W., Lu, Y., Brasch, R. C. Correlation of dynamic contrast-enhanced MR imaging with histologic tumor grade: Comparison of macromolecular and small-molecular contrast media. *AJR Am. J. Roentgenol. 171*, 941-949 (1998).
20. Su, M. Y., Jao, J. C., Nalcioglu, O. Measurement of vascular volume fraction and blood-tissue permeability constants with a pharmacokinetic model: Studies in rat muscle tumors with dynamic Gd-DTPA enhanced MRI. *Magn. Reson. Med. 32*, 714-724 (1994).
21. Su, M. Y., Muhler, A., Lao, X., Nalcioglu, O. Tumor characterization with dynamic contrast-enhanced MRI using MR contrast agents of various molecular weights. *Magn. Reson. Med. 39*, 259-269 (1998).
22. Brasch, R., Turetschek, K. MRI characterization of tumors and grading angiogenesis using macromolecular contrast media: Status report. *Eur. J. Radiol. 34*, 148-155 (2000).
23. Esserman, L., Kaplan, E., Partridge, S., Tripathy, D., Rugo, H., Park, J., Hwang, S., Kuerer, H., Sudilovsk, D., Lu, Y., Hylton, N. MRI phenotype is associated with response to doxorubicin and cyclophosphamide neoadjuvant chemotherapy in stage III breast cancer. *Ann. Surg. Oncol. 8*, 549-559 (2001).
24. Fletcher, B. D., Hanna, S. L., Fairclough, D. L., Gronemeyer, S. A. Pediatric musculoskeletal tumors: Use of dynamic, contrast-enhanced MR imaging to monitor responses to chemotherapy. *Radiology 184*, 243-248 (1992).
25. Bonnerot, V., Charpentier, A., Frouin, F., Kalifa, C., Vanel, D., Di Paola, R. Factor analysis of dynamic magnetic resonance imaging in predicting the response of osteosarcoma to chemotherapy. *Invest. Radiol. 27*, 847-855 (1992).
26. Hawighorst, H., Essig, M., Debus, J., Knopp, M. V., Engenhart-Cabilic, R., Schonberg, S. O., Brix, G., Zuna, I., van Kaick, G. Serial MR imaging of intracranial metastases after radiosurgery. *Magn. Reson. Imaging 15*, 1121-1132 (1997).
27. Hawighorst, H., Engenhart, R., Knopp, M. V., Brix, G., Grandy, M., Essig, M., Miltner, P., Zuna, I., Fuss, M., van Kaick, G. Intracranial meningeomas: Time- and dose-dependent effects of irradiation on tumor microcirculation monitored by dynamic MR imaging. *Magn. Reson. Imaging 15*, 423-432 (1997).

Date Received: September 15, 2002

Reprinted from *Analytical and Quantitative Cytology and Histology*
Vol.24 No.1, February 2002

Measuring Microvascular Density in Tumors by Digital Dissection

Michael Samoszuk, M.D., **Leonard Leonor,** B.S., **Froilan Espinoza,** M.D., **Philip M. Carpenter,** M.D., **Orhan Nalcioglu,** Ph.D., and **Min-Ying Su,** Ph.D.

OBJECTIVE: To develop and validate a digital dissection technique for measuring the cross-sectional area of blood vessels in histologic sections of tumors routinely stained with hematoxylin and eosin.
STUDY DESIGN: The procedure was first validated in four experimental tumors in rats by comparing the results of the digital dissection technique to functional estimates of the blood volume in the tumors as measured by dynamic, contrast-enhanced magnetic resonance imaging. The method was then tested on a variety of experimental and human tumors.
RESULTS: The digital dissection technique yielded results that exactly matched the functional measurements of blood volume in four experimental tumors. Digital dissection of 40 additional tumors in rats showed that 21 infiltrating ductal carcinomas had significantly greater microvascular density (MVD) than 19 benign fibroadenomas (12% vs. 7.9%, P = .028 by two-tailed t *test). In 10 human breast carcinomas the MVD was consistently greater than the measurement of blood vessel density as identified by immunohistochemical staining for factor VIII. The between-run coefficients of variation for the MVD assay were 12% (n=5) for a human breast cancer and 18% (n = 5) for an experimental rat tumor.*
CONCLUSION: The digital dissection technique is a reproducible, objective and accurate method of measuring MVD in sections of tumors that are routinely stained with hematoxylin and eosin. (Analyt Quant Cytol Histol 2002;24:15–22)

Keywords: blood vessels; angiogenesis, pathologic; image analysis, computer-assisted; magnetic resonance imaging; microvascular density; digital dissection.

Intratumoral microvascular density (MVD) has been proposed as a prognostic factor in various types of cancer and as a potential marker for treat-

From the Hematology-Oncology Center, Quest Diagnostics, Inc., San Juan Capistrano, and the Department of Pathology and Health Sciences Research Imaging Center, University of California–Irvine, Orange, California, U.S.A.

Dr. Samoszuk is Medical Director, Hematology-Oncology Center, Quest Diagnostics, Inc., and Associate Professor, Department of Pathology, University of California–Irvine.

Mr. Leonor is Research Assistant, Health Sciences Research Imaging Center, University of California–Irvine.

Dr. Espinoza is Pathologist, Hematology-Oncology Center, Quest Diagnostics, Inc.

Dr. Carpenter is Associate Professor, Department of Pathology, University of California–Irvine.

Dr. Nalcioglu is Director, Health Sciences Research Imaging Center, University of California–Irvine.

Dr. Su is Assistant Professor, Health Sciences Research Imaging Center, University of California–Irvine.

Supported in part by PHS grant R21CA86215 from the National Cancer Institute.

Address reprint requests to: Michael Samoszuk, M.D., Pathology Department, University of Californi–Irvine, Building 10 Route 40, UCI Medical Center, 101 The City Drive, Orange, California 92868-3298 (msamoszu@uci.edu).

Financial Disclosure: The authors have no connection to any companies or products mentioned in this article.

Received for publication September 7, 2001.

Accepted for publication November 28, 2001.

0884-6812/02/2401-0015/$15.00/0

ments that target blood vessels in cancer.[23,24]. Because angiogenesis is typically heterogeneous throughout tumors, it is often difficult to assess overall MVD by manually counting blood vessels in only a few selected portions of tumors.[4] This difficulty in measuring MVD accurately may account for some of the earlier conflicting reports regarding the clinical significance of MVD in breast,[14] prostate[1,9] and thyroid cancer.[2]

A number of methods have been described for measuring intratumoral MVD. One of the first methods involved assessment of neovascular "hot spots" highlighted with anti–factor VIII antibody.[24] Subsequent studies suggested that CD31 and CD34 might be better markers for identifying blood vessels in tumors.[6,22] The wide variation in methods and results eventually prompted an international consensus meeting to develop specific recommendations for the methodology and criteria for evaluating of MVD.[22] More recently, digital image analysis of breast cancer sections stained with monoclonal antibody to factor VIII has been proposed as a procedure for MVD.[5]

In order to be useful and accurate, histologic techniques for measuring MVD must ultimately be validated against an independent, noninvasive, functional measurement of blood flow within the tumor because the blood flow in a tumor is presumably related to MVD as well as to other factors. One such functional method of sampling blood vessels of an entire tumor and of estimating angiogenic activity employs contrast-enhanced magnetic resonance imaging (MRI).[21] Other methods of assessing the functional status of tumor microvasculature include color-coded Doppler flow measurement,[15] positron emission tomography[7] and uptake of albumin–Evan's blue dye.[10]

Of these methods, MRI now appears to be the preferred functional assay for assessing blood vessel density within tumors.[3,11] However, the signal enhancement measured by MRI is a function of many variables besides blood vessel density, including the amount of the contrast agent, relative perfusion of the tumor and microvascular permeability within the tumor.[18] For example, in order to measure blood volume in tissues more accurately by MRI, it is important to use a blood pool contrast agent that remains in the vasculature rather than a small contrast agent that quickly leaks into the interstitial space. For that reason, we used a macromolecular agent (albumin-Gd-DTPA) in the MRI studies described below.

In this report, we describe a semiautomated, electronic procedure for directly measuring the cross-sectional area of blood vessels in routinely stained histologic sections of tumors. The procedure employs rapid "digital dissection" of a two-dimensional image of the tumor to select and measure only the blood vessels within the tumor. The term *digital dissection* refers to a semiautomated procedure in which an imaging software program electronically identifies and measures blood vessels after an experienced operator digitally defines the color of the blood vessels and, in some cases, the region of interest. Results are expressed as a percentage of the total surface area of the section occupied by blood vessels. Below we demonstrate that this morphometric approach produces reproducible results that match those generated by functional MRI assessments of blood perfusion in tumors.

Materials and Methods

Digital Dissection Procedure

All studies were performed on tissues that were fixed in neutral buffered formalin and embedded in paraffin blocks in the usual manner. Sections of the tumors were cut at 5-μm thickness and stained with hematoxylin and eosin prior to analysis.

Each tumor was evaluated independently by two pathologists, who recorded 10 digital images at 40× from each slide using a Nikon Eclipse E600 microscope (Garden City, Long Island, New York, U.S.A.) equipped with a Spot digital camera (Diagnostic Instruments Inc., Sterling Heights, Michigan, U.S.A.). A typical slide included two to four different sections of the tumor. Each image represented a randomly selected, nonoverlapping region of tumor and connective tissue.

The individual images were then digitally dissected and analyzed using Image-Pro Plus, version 4, image analysis software (Media Cybernetics, Silver Spring, Maryland, U.S.A.). In order to select blood vessels for measurement, we used cubes of defined red, green and blue (RGB) values that ranged from 0 to 256 for each color. These RGB color values were assaigned by the software and were defined by the color of red blood cells in the image and by the color of empty space in the blood vessels. Generally each image required at least three cube values for assessment. For red blood cells, the RGB values ranged from approximately 176,43,85 to 239,99,134. Thus, we defined the criteria for intravascular space measurement as a combination of red blood cells and clear areas devoid of

staining. By defining RGB values for each tissue in this manner, we could compensate for any significant variations in fixation or staining quality.

These criteria do not necessarily include very small blood vessels or exclude lymphatic vascular channels without red blood cells. In practice, however, our preliminary studies indicated that such "lymphatic" channels or small blood vessels without red blood cells generally constituted significantly less than 10% of the total MVD in a typical microscopic field (data not shown). Hence, no correction was applied to compensate for possible lymphatic vessels or for undercounting of small vessels. We think that this decision was appropriate and justifiable because there are no objective criteria at this time to identify small empty blood vessels or open, lymphatic vessels.

In some cases the RGB values of red blood cells and empty blood vessel space overlapped with the color of necrotic debris, glandular lumen or fat. For this reason, we found it necessary, in approximately 25% of images, to have an experienced pathologist define a region of interest using a tool that was incorporated into the software. When set for an "irregular" area, this tool permitted the pathologist to define an area of any shape within the image to which the RGB values would be applied. Essentially, the tool digitally dissected the region of interest away from potentially interfering portions of the image.

After the operator defined the RGB values (and, in some cases, the area of interest), the statistical program accompanying the image analysis software then counted the number of pixels with the defined RGB values within the defined area. The average number of pixels corresponding to red blood cells and vessel lumens was then calculated for the 10 representative fields from each tumor. Because there are 1,358,395 pixels in the image array for the Spot camera, we then calculated the ratio of blood vessel pixels to total pixels in the image. This ratio represented the proportion of the total surface area of the image that was occupied by blood vessels and was a two-dimensional approximation of MVD. The results were multiplied by a factor of 100 in order to represent the percentage of the area of the image occupied by cross-sections of blood vessels.

Tumors

For animal studies, the malignant and benign breast tumors that we used were induced in rats by N-ethyl-N-nitrosourea, as previously described.[20] The four tumors that were used in the initial validation study were selected in order to cover a wide range of nuclear grade and differentiation, as measured by the Skarf-Bloom-Richardson (SBR) scale[20] (SBR grades ranging from 3 to 9). For factor VIII immunostaining studies, we used paraffin blocks from 10 randomly selected cases of human breast cancer that had been subjected to routine staining for estrogen receptors. One of these cases was then randomly selected for use in the reproducibility studies, along with one randomly selected experimental tumor from a rat.

Initial Validation Studies Using MRI

The MRI measurements of blood volume within the four tumors in rats used for the initial validation studies were performed exactly as described in a previous publication.[16] In brief, a macromolecular contrast agent (albumin-Gd-DTPA) was injected into the tail vein of the rats, and the time course of signal enhancement was measured in the tumor. Linear regression fitting was performed in order to fit the last 30 data points, and the blood volume was defined as the y-intercept in the best-fitting line.

Factor VIII Immunostaining

The 10 cases of human breast cancer were immunostained with monoclonal antibody to human factor VIII (Dako, Carpenteria, California, U.S.A.) using standard immunohistochemical staining techniques. For each tumor, we then acquired images of five nonoverlapping fields. These images were then analyzed with the Image Pro software. In brief, we manually traced the continuous outline of blood vessels that were stained with factor VIII antibody in each image, and the software then integrated the area of each image that was enclosed by a continuous tracing. Results were expressed as a percentage of the total surface area of each image.

Reproducibility Studies

The experimental rat tumor and human breast cancer were each reanalyzed by a single observer on five successive days. We then calculated the average MVD and coefficient of variation (interassay precision) for each tumor. To determine the effects of fixation, we examined tissues that had been fixed for 2, 4, 8 and 24 hours in neutral-buffered formalin or B-5 fixative. The effects of day-to-day variations in staining quality were assessed by cutting, staining and measuring sections of the same tissue on

five separate days. We also reviewed archival slides of human breast cancer that had been cut and stained at three outside institutions.

Results

Representative Digital Dissection of Microvessels in Tumors

Representative examples of the digital dissection of blood vessels in images from four different experimental tumors in rats are presented in Figure 1. The blood vessel lumens and red blood cells were electronically captured (indicated as a yellow pseudocolor) and quantified. An experienced operator completed the dissection and measurement of each representative microscopic field in less than two minutes. Using this technique, we could reliably identify and capture blood vessels as small in diameter as a few red blood cells (Figure 1F and H).

MRI Signal Enhancement Studies of Four Experimental Tumors

We previously showed that the peak signal enhancement in dynamic contrast-enhanced MRI is related to vascular density.[19] The results of dynamic contrast-enhanced MRI of four experimental rat tumors are presented in Figure 2. Tumor B clearly had a different enhancement kinetic pattern than the other three tumors. At early time points (first two time points after injection) it displayed slow enhancement, indicating low perfusion; at later times it showed a continuous enhancing pattern, indicating that the contrast agent was slowly leaking into the interstitial space due to high permeability of the microvessels. The blood volume was determined as the y-intercept by performing linear regression fitting to the last 30 data points, as previously described.[19] The intercept enhancement for tumor B was therefore determined to be 30, indicating the highest blood volume. Tumors D, A and C had signal enhancement intercepts of 18.3, 16.9 and 8.3, respectively. Thus, the rank order for blood volume in these four tumors was B > D > A > C.

The digital dissection procedure yielded an MVD of 6% for tumor B. For tumors D, A and C, the MVD values were 4%, 3.4% and 2.6%, respectively. Thus, the rank order of the tumors for MVD was B > D > A > C, exactly matching the rank order for the MRI signal enhancement. Identical rank order results were also obtained when a second pathologist independently performed the MVD procedure.

A linear regression analysis relating MVD to MRI results yielded $R^2 = .96$, with an F value of 62.1 (at three degrees of freedom) and a significance level of .03. We conclude, therefore, that the MVD procedure is valid because it consistently produced rank order results that exactly matched the rank order of functional measurements of blood volume in the four experimental tumors. Moreover, there was a relatively high degree of statistical correlation between MVD and the results of the MRI studies.

MVD in 40 Experimental Rat Tumors

The results of the measurement of MVD in 40 experimental rat tumors (21 infiltrating ductal carcinomas and 19 benign fibroadenomas) are presented in Figure 3. There was considerable overlap in MVD values for both categories of tumor. Nevertheless, the mean MVD for invasive carcinomas (11.9%) was significantly higher ($P = .028$ by a two-sample t test for the difference in the means of two samples, assuming equal variances) than the mean MVD for fibroadenomas (7.9%). These results are consistent with the finding of a previous report that invasive carcinomas generally have a greater blood perfusion than fibroadenomas when assessed by MRI, although there is substantial overlap in the MRI measurements as well.[20]

MVD and Factor VIII Areas in Human Breast Cancers

The relationship between MVD and factor VIII area in 10 human breast cancers is plotted in Figure 4. In every case, MVD exceeded the area of the tumor that was circumscribed by factor VIII immunostaining. Microscopic examination confirmed that factor VIII did not stain all the vascular channels that contained red blood cells within the tumors. Moreover, factor VIII staining was frequently discontinuous or faint, making it difficult to trace and measure the surface area bounded by factor VIII.

Reproducibility Studies

The between-run precision (coefficient of variation) of MVD measurement in a representative experimental tumor in a rat was 18% (n = 5). In a representative human breast cancer, the between-run precision was 12% (n = 5). The average interpathologist variation between two pathologists on four randomly selected cases was 15%.

Tissues that had been fixed in formalin for four or more hours uniformly yielded sections that could be reproducibly and easily evaluated by the digital dissection technique. Fixation for less than four

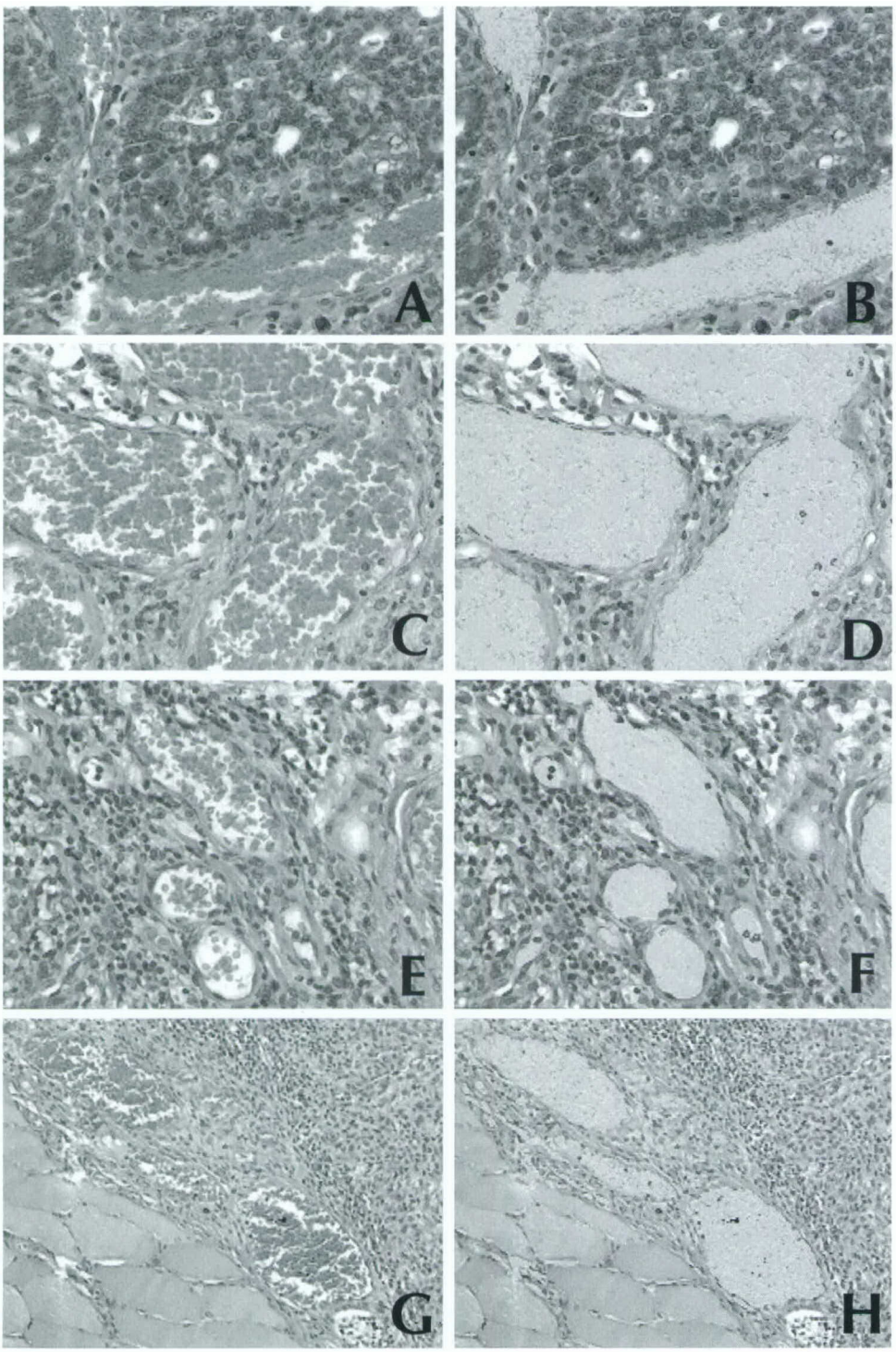

Figure 1 Digital dissection of blood vessels in representative sections from four different tumors in rats. After the RGB values for red blood cells and lumenal spaces were defined by the operator, the software automatically selected the blood vessels within the images (indicated by yellow pseudocolor) and counted the number of pixels within the selected regions. Figures A, C, E and G are images of sections that were routinely stained with hematoxylin and eosin. Figures B, D, F and H are the corresponding images that were digitally dissected for microvessels. Note the very small blood vessels in F and H (×40).

hours often yielded substantial retraction artifact that severely interfered with interpretation. Tissues that were properly fixed in B-5 produced results that were equivalent to those after fixation in formalin. The variation attributable to day-to-day differences in staining with hematoxylin and eosin was approximately 6%. Archival slides stained at three other institutions were also readily interpret-

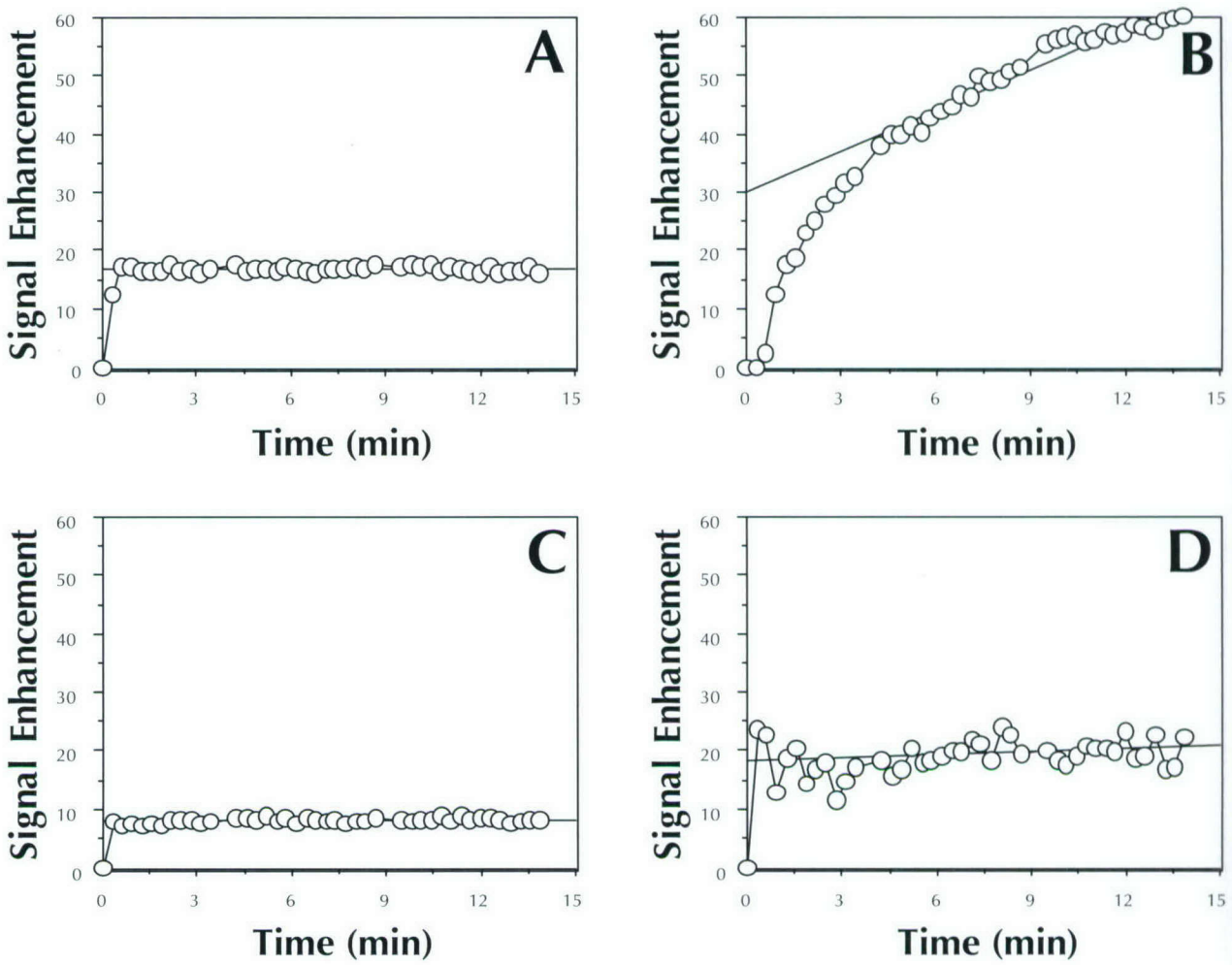

Figure 2 Signal enhancements after injection of albumin-Gd-DTPA, measured by MRI in four experimental tumors. The intercept for the linear regression fitting to the last 30 data points was used as the blood volume index. The tumor in (B) had the highest intercept enhancement (30.1). The tumor in (C) had the lowest intercept enhancement (8.3). The intercept enhancements for tumors (A) and (D) were 16.9 and 18.3, respectively. Thus, the rank order for blood volume was B > D > A > C.

ed by this method when the RGB values were reset for each slide in order to compensate for variations in staining quality.

Discussion

In this report we describe a new, semiautomated procedure for measuring MVD in tumors. Unlike previously described methods of measuring MVD, our procedure was first validated against a functional indicator of blood flow in tumors (dynamic contrast-enhanced MRI) that presumably was related to MVD. Our morphometric approach has a high degree of precision (coefficient of variation < 20%) and is easily and rapidly performed (usually less than two minutes per image). Furthermore, the method that we describe does not rely upon the immunohistochemical identification of specific vascular endothelial markers or the manual counting of blood vessels.

Measurement of MVD in tumors by any morphometric method is potentially subject to sampling errors due to the intrinsic heterogeneity in the distribution of blood vessels within a tumor.[17] Thus, optimum assessment of MVD by morphometry requires analysis of multiple images and sections of the tumor in order to gain a truly accurate and rep-

resentative measurement of the overall blood vessel density. For this reason, a semiautomated procedure (such as the one that we describe) is preferable to manual methods, especially when analyzing a large number of images.

A somewhat unexpected finding in this study was the apparent discordance between MVD, as measured by our digital dissection technique, vs. tracing of factor VIII staining. As mentioned above, much of this discrepancy may be attributed to the inherent technical difficulty in reproducibly identifying and tracing often-discontinuous staining for factor VIII. Another possible explanation is that factor VIII was not expressed on some of the vascular channels within the tumors that we studied because the endothelial cells lining the channels were themselves abnormal.[13] It is not clear if this phenomenon could also be related to the concept of vasculogenic mimicry that was previously described for uveal melanomas.[8,12]

Additional studies will be needed in order to characterize more fully the types of vascular channels that are identified in tumors by different staining techniques (factor VIII, CD31, CD34) and by the digital dissection procedure that we describe above. In the meantime, the digital dissection procedure has the advantage of identifying and measuring all vascular channels that contain red blood cells, regardless of the presence or absence of endothelial cell markers. Thus, digital dissection should prove useful in future studies of the biology of blood vessels in tumors.

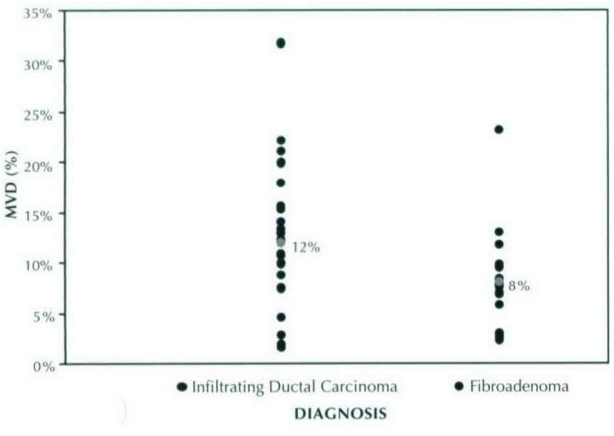

Figure 3 Comparison of MVD in infiltrating ductal carcinomas and fibroadenomas in rats. The mean MVD of the carcinomas was significantly higher ($P < .05$) than the mean MVD of fibroadenomas.

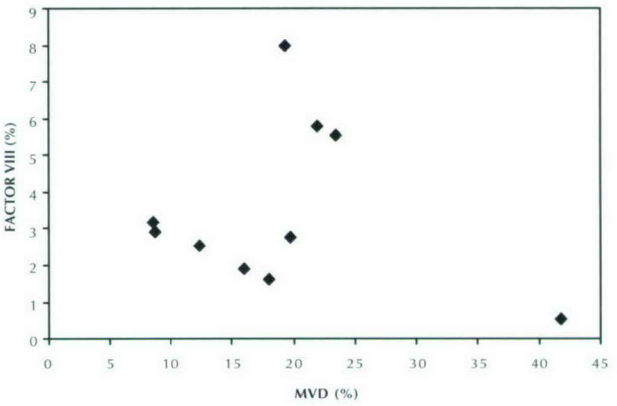

Figure 4 Comparison of MVD to factor VIII staining in 10 human breast cancers. In every case, MVD was greater than the surface area enclosed by factor VIII immunostaining.

References

1. Abdulkadir SA, Carvalhal GF, Kaleem Z: Tissue factor expression and angiogenesis in human prostate carcinoma. Hum Pathol 2000;31:443–447
2. Akslen LA, LiVolsi VA: Increased angiogenesis in papillary thyroid carcinoma but lack of prognostic importance. Hum Pathol 2000;31:439–442
3. Brasch R, Turetschek K: MRI characterization of tumors and grading angiogenesis using macromolecular contrast media: Status report. Eur J Radiol 2000;34:148–155
4. Costello P, McCann A, Carney DN, Dervan PA: Prognostic significance of microvessel density in lymph node negative breast carcinoma. Hum Pathol 1995;26:1181–1184
5. Cruz D, Valenti C, Dias A, Seixas M, Schmitt F: Microvessel density counting in breast cancer: Slides vs. digital images. Analyt Quant Cytol Histol 2001;23:15–20
6. de la Taille A, Katz AE, Bagiella E, Buttyan R, Sharir S, Olsson CA, Burchardt T, Ennis RD, Rubin MA: Microvessel density as a predictor of PSA recurrence after radical prostatectomy: A comparison of CD34 and CD31. Am J Clin Pathol 2000;113:555–562
7. Fanelli M, Locopo N, Gattuso D, Gasparini G: Assessment of tumor vascularization: Immunohistochemical and non-invasive methods. Int J Biol Markers 1999;14:218–231
8. Folberg R, Hendrix MJ, Maniotis AJ: Vasculogenic mimicry and tumor angiogenesis. Am J Pathol 2000;156:361–381
9. Gettman MT, Pacelli A, Slezak J, Bergstralh EJ, Blute M, Zincke H, Bostwick DG: Role of microvessel density in predicting recurrence in pathologic stage T3 prostatic adenocarcinoma. Urology 1999;54:479–485
10. Graff BA, Bjornaes I, Rofstad EK: Macromolecule uptake in human melanoma xenografts: Relationships to blood supply, vascular density, microvessel permeability and extracellular volume fraction. Eur J Cancer 2000;36:1433–1440
11. Jensen JH, Chandra R: MR imaging of microvasculature. Magn Reson Med 2000;44:224–230

12. Maniotis AJ, Folberg R, Hess A, Seftor EA, Gardner LM, Pe'er J, Trent JM, Meltzer PS, Hendrix MJ: Vascular channel formation by human melanoma cells in vivo and in vitro: Vasculogenic mimicry. Am J Pathol 1999;155:739–752
13. McDonald DM, Foss AJ: Endothelial cells of tumor vessels: Abnormal but not absent. Cancer Metastasis Rev 2000;19: 109–120
14. Medri L, Nanni O, Volpi A, Scarpi E, Dubini A, Riccobon A, Becciolin A, Bianchi S, Amadori D: Tumor microvessel density and prognosis in node-negative breast cancer. Int J Cancer 2000;89:74–80
15. Peters-Engl C, Medl M, Mirau M, Wanner C, Bilgi S, Sevelda P, Obermair A: Color-coded and spectral Doppler flow in breast carcinomas: Relationship with the tumor microvasculature. Breast Cancer Res Treat 1998;47:83–89
16. Samoszuk MK, Su MY, Najafi A, Nalcioglu O: Selective thrombosis of tumor blood vessels in mammary adenocarcinoma implants in rats. Am J Pathol 2001;159:245–251
17. Schor AM, Pazouki S, Morris J, Smither RL, Chandrachud LM, Pendleton N: Heterogeneity in microvascular density in lung tumours: Comparison with normal bronchus. Br J Cancer 1998;77:946–951
18. Su MY, Muehler A, Lao X, Nalcioglu O: Tumor characterization with dynamic contrast-enhanced MRI using MR contrast agents of various molecular weights. Magn Reson Med 1998;39:259–269
19. Su MY, Najafi A, Nalcioglu O: Regional comparison of tumor vascularity and permeability parameters measured by albumin-Gd-DTPA and Gd-DTPA. Magn Reson Med 1995;34:402–411
20. Su MY, Wang Z, Carpenter P, Lao X, Muhler A, Nalcioglu O: Characterization of N-ethyl-N-nitrosourea-induced malignant and benign breast tumors in rats by using three MR contrast agents. J Magn Reson Imaging 1999;9:177–186
21. van Dijke CF, Brasch RC, Roberts TP, Weidner N, Mathur A, Shames DM, Mann JS, Demsar F, Lang P, Schwickert HC: Mammary carcinoma model: Correlation of macromolecular contrast-enhanced MR imaging characterizations of tumor microvasculature and histologic capillary density. Radiology 1996;198:813–818
22. Vermeulen PB, Gasparini G, Fox SB, Toi M, Martin L, McCulloch P, Pezzella F, Viale G, Weidner N, Harris AL, Dirix LY: Quantification of angiogenesis in solid human tumours: An international consensus on the methodology and criteria of evaluation. Eur J Cancer 1996;32A:2474–2484
23. Weidner N: Current pathologic methods for measuring intratumoral microvessel density within breast carcinoma and other solid tumors. Breast Cancer Res Treat 1995;36: 169–180
24. Weidner N: Intratumor microvessel density as a prognostic factor in cancer. Am J Pathol 1995;147:9–19

Monitoring Chemotherapy Induced Changes in the Carcinogen ENU Induced Infiltrating Ductal Adenocarcinoma and Non-Infiltrating Papillary Adenocarcinoma by Longitudinal MRI studies

M-Y. Su[1], M. J. Hamamura[1], H. Wang[1], H. J. Yu[1], J. Wang[1], P. M. Carpenter[2], O. Nalcioglu[1]

[1]Center for Functional Onco-Imaging, University of California, Irvine, CA, United States, [2]Department of Pathology, University of Caifornia, Irvine, CA, United States

Purpose

It is well known that carcinogen ENU can induce benign and malignant tumors. In this study we utilized this wide variation of tumor types and tumor grades to simulate human breast cancer, and studied their response to chemotherapy (Taxotere). Longitudinal MRI was applied to measure the tumor volume and the contrast enhancement kinetics of a small extracellular agent Gd-DTPA-BMA and a medium size blood pool agent Gadomer-17. We investigated whether the vascular parameters measured by contrast enhanced MRI at an early time can differentiate responders from non-responders at later times, thus to predict therapy outcome.

Methods

53 Sprague-Dawley rats were injected with 90 mg/kg carcinogen ENU (N-ethyl-N-nitrosourea). Forty seven mammary tumors appeared within 9 months, and 35 tumors grew to 1.0 cm for the MRI study, which included 23 infiltrating ductal adenocarcinoma (IDC), 3 non-infiltrating papillary adenocarcinoma (NPC), 7 fibroadenoma (FA), 1 Sclerosing adenosis, and 1 papilloma. The baseline MRI was conducted when the tumor reached 1 cm. The imaging protocol included a T2-weighted sequence for volumetric measurement, and the dynamic study using a small molecular weight agent Gd-DTPA-BMA (®Omniscan, 0.1 mmol/kg), followed by an intermediate molecular weight agent Gadomer-17 (0.05 mmol/kg, provided by Schering AG, Germany). After the MRI study was completed the rats received i.v. injection of 4 mg/kg Taxotere. Three follow-up MRI studies were performed, once per week (noted as W1, W2, and W3). The rats continued to receive weekly Taxotere treatment after each MRI study. The volume of each tumor was measured, and depending on the volumes at W3 compared to the baseline, the tumors were separated into responders (volume decreased by 50%), non-responders (volume increased by 50%), and stabilizer (others). Also, the response at each time point compared to the baseline was analyzed. The MRI enhancement parameters (at 30 sec, 1-min, and 2-min) and the K21 decay rate were used to investigate whether any of these parameters themselves, or the changes compared to the previous time measures, can be used to differentiate responders from non-responders at a later time.

Results

Among these 35 tumors, 29 tumors (20 IDC, 3 NPC, 4 FA, 1 adenosis, and 1 papilloma) have completed the longitudinal study at 4 time points. According to the tumor volume at the end of week-3 compared to the baseline (noted as GR), the tumor was classified into responder (GR < 0.5), stabilizer (0.5 < GR <1.5), and non-responder (GR > 1.5). Of the 20 IDC, 9 were responders, 5 were stabilizers, and 6 were non-responders. Interestingly all 3 NPC were stabilizer. Three fibroadenomas were non-responders and only one FA was a responder. Figure 1 shows the T2-weighted images and the contrast enhancement kinetics from an IDC which showed a consistent regression. Figure 2 shows another IDC which grew larger over time. However, not every tumor was responding consistently. Given the complicated response pattern, the statistical analysis was only performed for IDC and the response at each time point was analyzed separately. Tumor size at week-1 compared to the baseline was calculated, and separated into +/- growth groups. Among all 8 MRI parameters, the baseline Gadomer-17 enhancements at 1-min and 2-min at baseline showed a significant difference ($p < 0.05$, Wilcoxon rank-sum tests) between the 2 groups with +/- growth at week-1. The same analysis was applied at week-2 and week-3, but no MRI parameters revealed a significant difference between different growth groups at week-2 and week-3.

One responder (infiltrating ductal adenocarcinoma)

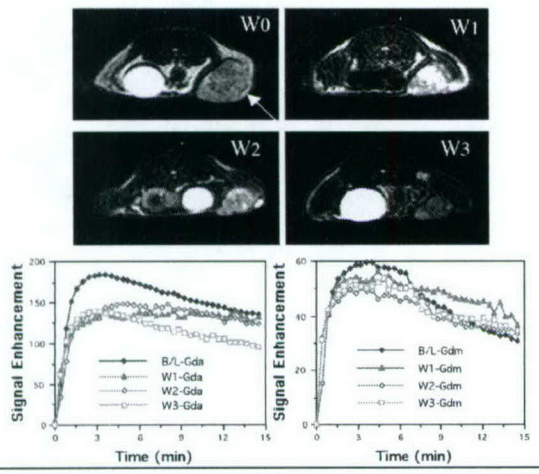

Figure 1: The T2-weighted image, and the enhancement kinetics measured by Gd-DTPA-BMA(left) and Gadomer-17(right) in one responder tumor (infiltrating ductal adenocarcinoma). The tumor showed continuous regression over time. The kinetics measured by Gd-DTPA-BMA showed reduced intensity after the first treatment, and the pattern of the curve became more flattened (i.e. no wash-out).

One non-responder (infiltrating ductal adenocarcinoma)

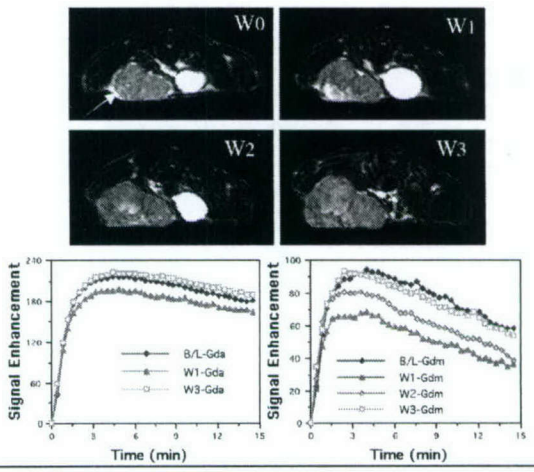

Figure 2: The T2-weighted image, and the enhancement kinetics measured by Gd-DTPA-BMA(L) and Gadomer-17(R) in one non-responder tumor (infiltrating ductal adenocarcinoma). Apparently the tumor grew larger and larger over time. The Gd-DTPA-BMA kinetics were similar over time, and Gadomer-17 kinetics showed a great reduction at week-1 then recovered to the baseline level at week-3.

Discussion

The volumetric changes and contrast enhancement changes in ENU induced tumors receiving Taxotere were measured by longitudinal MRI. ENU induced benign and malignant tumors (came with 2 major types, infiltrating ductal adenocarcinoma, and non-infiltrating papillary adenocarcinoma simulating in-situ cancers). Among all tests, only the baseline Gadomer-17 enhancements at 1-min and 2-min revealed a significant difference between IDC's which grew bigger at week-1 versus those which shrank at week-1. This maybe interpreted as that tumors with a higher vascularity measured by Gadomer-17 had a better response (shrinkage), possibly due to more drug delivery. The data also indicated that although ENU induced tumors came with a large variation, they also showed different responses to therapy. Although ENU induced tumors may simulate the variety in human breast cancer, but it may not be a good tumor model for drug response testing.

Acknowledgement This work was supported in part by a grant from DOD ARMY BCRP No. DAMD17-01-0178.

Characterization of Angiogenesis in The Carcinogen ENU Induced Benign And Malignant Mammary Tumor Model

Min-Ying Su, Hon Yu, Jun Wang, Phillip Carpenter[2], John Fruehauf[3], and Orhan Nalcioglu
Center for Functional Onco-Imaging and [2]Department of Pathology, University of California, Irvine, CA and [3]Oncotech Inc. Tustin, CA

Synopsis

Angiogenesis in carcinogen ENU-induced benign and malignant tumor models were studied with dynamic contrast enhanced MRI using two contrast agents (Gadodiamide and Gadomer-17). The tumors were then excised for immunohistochemical (IHC) staining to measure expression of angiogenic biomarkers, including mutant p53, TSP-1, VEGF, and Factor VIII microvessel density. Benign and malignant tumors had distinct contrast enhancement kinetics. Malignant tumors had a higher microvessel density than benign tumors. MRI and IHC may provide different aspects (macroscopic and microscopic) complementing each other for assessment of tumor angiogenesis.

Purpose

As the potential of anti-angiogenic or anti-vascular therapy for cancer treatment becomes more promising, the development of valid animal models as well as therapeutic efficacy markers have become increasingly important. The carcinogen ENU can induce benign and malignant tumors in rats, and the malignant tumors came with various SBR (Scarff-Bloom-Richardson) grades, thus it can be used as a suitable model for studies of angiogenesis. We applied dynamic contrast enhanced MRI and immunohistochemical (IHC) staining to study angiogenesis in the benign and malignant tumors of this model. Assessment of angiogenic biomarkers by immunohistochemical (IHC) staining is the most commonly used technique. For each specimen, we measured the expression level of mutant p53 (mp53), thrombospondin-1 (TSP-1), Vascular Endothelial Growth Factor (VEGF), and microvessel density (MVD) using Factor VIII staining. On the other hand, contrast enhanced imaging can be applied to measure the vascularity non-invasively. We utilized the broad spectrum of the ENU induced mammary tumor model and compared the angiogenesis measured using MRI and IHC molecular markers. Proper validation of imaging technique will facilitate its application in therapy monitoring, especially for anti-angiogenic or anti-vascular therapies.

Methods

N-ethyl-N-nitrosourea (ENU, 90 mg/kg) was injected i.p. into 30-day old SPF Sprague-Dawley rats (n=50) to induce mammary tumors. The tumors started to appear 2 months after injection. The baseline MRI study was performed when the tumor reached approximately 1.0 cm in diameter. For each tumor the enhancement kinetics of two contrast agents, the small agent Gadodiamide (Omniscan, 0.1 mmol/kg) and a mid-sized agent Gadomer-17 (0.05 mmol/kg, kindly provided by Schering AG, Germany), were measured. The volumetric growth rates, as well as the early (30-sec) and maximum (approximately 2-min) enhancements between benign and malignant tumors were compared. Each tumor was then surgically removed for IHC staining analysis to measure the expression of mp53, TSP-1, VEGF, and MVD. The rats were kept for observation of recurrence and further development of other tumors. The tumor types and angiogenesis of primary and subsequently developed tumors were compared.

Results

Ninety three tumors were found within 1 year after the injection of ENU. Most tumors belonged to four major types, 2 malignant and 2 benign. The malignant tumors included ductal adenocarcinoma (n=25) and papillary adenocarcinoma (n=21), and the two major benign lesions were fibroadenoma (n=24) and adenosis (n=13). Multiple tumors (up to 5) could develop in one rat, all at different locations. No tumor recurrence was observed at the surgical site after removal of a previous tumor. The subsequently developed tumors were not associated with the primary tumor. In MRI studies, two malignant tumors exhibited similar enhancement kinetics, showing rapid early enhancing slope and high enhancement magnitude. Figure 1 shows the enhancement kinetics measured by Gadodiamide (a) and Gadomer-17 (b) from these 4 tumor types. Two benign lesions had much slower early enhancing slope (highly significantly). The volumetric growth rates showed large variations even within each tumor type, and they were not correlated with the enhancement kinetics of both studied contrast agents. In IHC studies, the ductal adenocarcinoma had the highest microvessel density, then in order were papillary adenocarcinoma, fibroadenoma, and adenosis had the lowest microvessel density. All tumors had wild type p53. VEGF and TSP-1 were not significantly different among the 4 types. Higher vessel density was associated with higher MRI enhancement. Table 1 summarizes the growth rates, 30-sec and 2-min MR contrast enhancements and the IHC data.

Table 1: The growth rate, Gadodiamide and Gadomer-17 enhancements at 30-sec and 2-min and the IHC biomarkers: factor VIII microvessel density, VEGF histo-score and TSP-1 optical density in 4 tumor types

	Ductal AC	Papillary AC	FA	Adenosis
GR (cc/day)	0.06 – 0.13	0.07 – 0.14	0.03 – 0.03	0.05 – 0.06
Gadodiamide @30s	122 – 62	126 – 68	39 – 14	57 – 22
Gadodiamide @2min	251 – 69	240 – 75	145 – 54	204 – 65
Gadomer-17 @30s	47 – 30	52 – 23	23 – 10	24 – 11
Gadomer-17 @2min	92 – 40	96 – 32	51 – 19	73 – 22
Factor VIII MVD	**79 – 19**	**70 – 20**	**58 – 18**	**53 – 17**
VEGF H-score	134 – 98	74 – 68	126 – 144	50 – 76
TSP-1	62 – 22	60 – 23	57 – 27	59 – 21

Discussion

A better characterization of this model may aid in future development of diagnostic or therapeutic agents tested on this model. As in human breast tumors, the enhancement kinetics of malignant tumors had a rapid up-slope, reaching to the maximum quickly, followed by a wash-out phase. The early enhancement is the best parameter to differentiate benign from malignant tumors. The immunohistochemical staining was used to measure the angiogenic biomarkers. The ductal adenocarcinoma had the highest microvessel density, then in order were papillary adenocarcinoma, fibroadenoma, and the adenosis had the lowest microvessel density, which was consistent with the degree of malignancy and benignity. MRI and IHC data were not correlated with each other, which may be due to the problem of tumor heterogeneity and non-matching sampling. However, MRI and IHC may provide different aspects (macroscopic and microscopic) complementing each other for assessment of tumor angiogenesis.

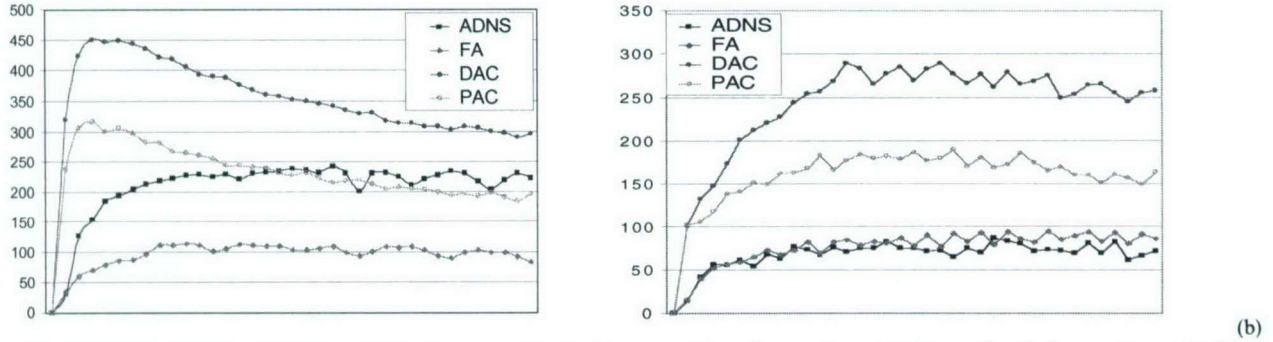

Figure 1: Examples of Gadodiamide (a) and Gadomer-17(b) enhancement kinetics for one papillary adenocarcinoma(PAC), one ductal adenocarcinoma(DAC), one adenosis(ADNS), and one fibroadenoma(FA). The malignant tumors had higher enhancements.

Acknowledgement

This work was supported in part by NIH/NCI CA86215 and the US ARMY BCRP grant number DAMD17-01-1-0178.

CHARACTERIZATION OF ANGIOGENESIS IN THE CARCINOGEN ENU INDUCED BENIGN AND MALIGNANT MAMMARY TUMOR MODEL

Min-Ying Su, PhD, Hon Yu, MS, Jun Wang, MD, and Orhan Nalcioglu, PhD

Center for Functional Onco-Imaging, University of California, Irvine CA 92697-5020

E-mail: msu@uci.edu

As the potential of anti-angiogenic or anti-vascular therapy for cancer treatment becomes more promising, the development of valid animal models as well as therapeutic efficacy markers have become increasingly important. The carcinogen ENU can induce benign and malignant tumors in rats, and the malignant tumors came with various SBR (Scarff-Bloom-Richardson) grades, thus it can be used a suitable model for studies of differential diagnosis as well as malignant tumor grade staging. Assessment of angiogenesis by immunohistochemical (IHC) staining is the most commonly used technique. For each specimen we measured the expression level of mutant p53, thrombospondin-1, Vascular Endothelial Growth Factor (VEGF), and microvessel density using Factor VIII staining. On the other hand, imaging may be complementary to the IHC studies to measure the vascularity. In this study we characterized the angiogenesis status of the ENU induced mammary tumor model using Magnetic Resonance Imaging (MRI) and IHC molecular markers.

N-ethyl-N-nitrosourea (ENU, 90 mg/kg) was injected i.p. into 30-day old SPF Sprague-Dawley rats (n=50) to induce mammary tumors. The tumors started to appear 2 months after injection. The baseline MRI study was performed when the tumor reached approximately 1.0 cm in diameter. For each tumor the enhancement kinetics of two contrast agents, the small agent Gd-DTPA and a mid-sized agent Gadomer-17, were measured. The volumetric growth rates, as well as the early (30-sec) and maximum (approximately 2-min) enhancements between benign and malignant tumors were compared. Each tumor was then surgically removed for IHC staining analysis. The rats were kept for observation of recurrence, further development of other tumors, and metastasis into other organs, to explore whether this model can be used to study recurrence and metastasis as in human breast cancer.

Ninety three tumors were found in 1 year after the injection of ENU. Most tumors belonged to four major types, 2 malignant and 2 benign. The malignant tumors included ductal adenocarcinoma (n=25) and papillary adenocarcinoma (n=21), and the two major benign lesions were fibroadenoma (n=24) and adenosis (n=13). Multiple tumors (up to 5) could develop in one rat, all at different locations. Interestingly no tumor recurrence was observed at the surgical site after removal of a previous tumor. Also, none of the abdominal tumors were from breast origin. We also investigated lymph nodes from some rats, and found no sign of any cancer. In MRI studies, the two malignant tumors exhibited similar enhancement kinetics, showing rapid early enhancing slope and high enhancement magnitude. The two benign lesions had much slower early enhancing slope (highly significantly). In IHC studies, the ductal adenocarcinoma had the highest microvessel density, then in order was papillary adenocarcinoma, fibroadenoma, and the adenosis had the lowest microvessel density. All tumors had wild type p53. VEGF and TSP-1 were not significantly different among the 4 types. Higher vessel density was associated with higher MRI enhancement.

Our results demonstrated that all carcinogen ENU induced tumors were primary tumors, and they did not metastasize to lymph nodes or to other organs. A better characterization of this model may aid in future development of diagnostic or therapeutic agents tested on this model.

The U.S. Army Medical Research Materiel Command under DAMD17-01-1-0178 supported this work.

Quantitative Vascular Density Assessed by a Semiautomatic Histological Method in Comparison with MRI Enhancements in Carcinogen Induced Benign and Malignant Mammary Tumors in Rats

Min-Ying Su, Michael Samoszuk[2], Leonard Leoner, Phillip M. Carpenter[2], and Orhan Nalcioglu
Center for Functional Onco-Imaging, and [2]Department of Pathology, University of California-Irvine, CA, USA

Abstract

The development of therapeutic efficacy markers for anti-angiogenic or anti-vascular therapy is in great need. Assessment of microvascular density by immunohistochemical staining is the most commonly used technique. Imaging can provide a through sampling, but to date there is not a suitable agent and technique whose accuracy has been validated. In this study, we developed a semi-automatic histological analysis method to quantitatively measure the cross-sectional area of vessels in carcinogen ENU induced benign and malignant tumors. The results were compared to enhancements measured by three contrast agents, Gd-DTPA, Gadomer-17, and albumin-Gd-DTPA.

Purpose

As the potential of anti-angiogenic or anti-vascular therapy for cancer treatment becomes more promising, there is an ever increasing need for the development of therapeutic efficacy markers. Assessment of microvascular density by immunohistochemical staining is the most commonly used technique. However, the accuracy is greatly dependent on successful staining of endothelial cells and highly subjective to the heterogeneity. In this study we analyzed the vascular density in a carcinogen induced mammary tumor model, including malignant tumors of various SBR (Scarff-Bloom-Richardson) grades and benign tumors [Stoica et al. Anticancer Research 4:5, 1984]. We have previously reported the characteristics of these tumors studied by dynamic contrast enhanced MRI by using three contrast agents of various molecular weights [Su et al. JMRI 9:177-186, 1999]. The results indicated that the enhancement kinetics measured by the largest agent Albumin-Gd-DTPA in the high-grade infiltrating ductal carcinoma (IDC) has a higher vascular volume and permeability than that in the low-grade IDC, and fibroadenoma has the lowest vascular volume. In this study we performed quantitative vascular density measurements from the tumor specimens included in that study and investigated the association between the MRI results and the vessel density. A semiautomatic method was developed to measure the vascular area from the H&E stained histological slides. The vascular density between malignant tumors of different grades and 3 different types of benign tumors, fibroadenoma, tubular adenoma and papiloma were also compared.

Methods

The carcinogen N-ethyl-N-nitrosourea (ENU, 45-180 mg/kg) was injected into 50 SPF Sprague-Dawley rats to induce mammary tumors. When the tumor had reached 1.5 cm in diameter, dynamic contrast enhanced MRI studies were carried out by using three agents, Gd-DTPA (0.1 mmol/kg), Gadomer-17 (0.05 mmol/kg), and albumin-Gd-DTPA (0.02 mmol/kg). Gadomer-17 was provided by Schering AG (Berlin, Germany), which is a synthetic dendrimeric gadolinium chelate with an apparent molecular weight of 35 kD. Albumin-Gd-DTPA had a molecular weight of 90 kD. The experiments were performed on a GE 1.5 T Signa scanner. The dynamic images were acquired by using a spin-echo pulse sequence with TR/TE=140/14 ms. Gd-DTPA was injected first, 1 hour later followed by Gadomer-17. Albumin-Gd-DTPA study was conducted on a different day. After the imaging studies were finished, the tumor was removed for pathological examination. For each tumor, tissue samples from 2-6 regions were examined. In the case of infiltrating ductal carcinoma, SBR grade was determined.

For quantitative assessment of vascular density, we developed a digital dissection technique to measure the cross-sectional area of blood vessels in histological sections of tumors. Five micron thickness section was cut then stained with H&E. Ten digital images at 40x power were recorded from each slide. Each image represented a randomly selected, non-overlapping region of tumor and connective tissue. The RGB color values were defined by the color of red blood cells in the image and by the color of the empty space in the blood vessels. The intravascular area was defined as a combination of red blood cells and clear areas devoid of any staining. To avoid contamination from necrotic debris, glandular lumen, or fat with same color-coding, it is necessary to have an experienced pathologist manually define a region of interest. After the RGB values and ROI were defined, the statistical program counted the number of pixels within the defined area to calculate the % vascular area. The results were compared among different types of lesions, and also correlated with the MRI enhancements measured by 3 contrast agents.

Results

The percent vascular area and the gray level enhancements at 3-min post contrast injection in different types of tumors, including infiltrating ductal carcinoma (IDC), fibroadenoma (FA), tubular adenoma (TA) and papiloma (PAP), are listed in table 1. Although tubular adenoma and papiloma were benign lesions, we found that these two tumors showed very strong enhancements. Interestingly they also had relatively high vascular density. In general, the IDC group had a significantly higher vascular density than the fibroadenoma (13±7 % vs. 8±5 %, $p < 0.05$). We also found 2 benign "epidermal inclusion cyst" in this study, which had a very low vascular area (less than 0.4%) as expected from the nature of the cyst, and also very low MRI enhancements. However, on a one-to-one basis, we failed to obtain a significant correlation between % vascular area and MRI enhancements measured by either of the 3 contrast agents used in this study.

Table 1: % vascular area and enhancements at 3-min post injection

	% Vascular	Gd-DTPA	Gadomer-17	Alb-Gd
IDC-LG (n=7)	13 ± 11 %	205 ± 33	112 ± 39	21 ± 11
IDC-MG (n=7)	14 ± 5 %	214 ± 65	168 ± 43	44 ± 15
IDC-HG (n=6)	13 ± 4 %	194 ± 62	181 ± 42	38 ± 13
FA (n=18)	8 ± 5 %	171 ± 47	103 ± 17	14 ± 10
TA (n=6)	14 ± 8 %	231 ± 61	175 ± 76	35 ± 5
PAP (n=3)	10 ± 6 %	276 ± 92	170 ± 54	38 ± 9

Discussion

A semiautomatic procedure was developed for quantitative measurements of vascular area in the H&E stained tumor slides. The advantage of this technique over the commonly used immunohistochemical staining using Factor-VIII, CD-31 or CD-34 is that it does not count on positive staining of endothelial cells. In addition, we may separately analyze the area occupied by the red blood cells vs. the empty lumen to obtain a measure of functional vessels in which the blood flows through. However, the problem of inadequate sampling still exists due to the nature of the analysis from thin histological sections as compared to the imaging study. Using a lower power field (e.g. 10x instead of 40x) may facilitate more adequate sampling. The difficulty in the investigation of correlation between vascular density and the MRI enhancements has long been recognized. Although the blood pool agent such as albumin-Gd-DTPA may provide a more accurate measurement of vascular volume, a substantial enhancement could be due to the leakage of agents into the interstitial space through vascular permeability. Accurate measurements of vascular volume/ permeability, either with imaging or histological methods, are in great need for the assessment of the therapeutic effect induced by anti-angiogenic (or, anti-vascular) agents.

Acknowledgement.

This work was supported in part by NIH grant # R21 CA86215.

Longitudinal Taxotere Chemotherapy Treatment Induced Vascular and Structural Changes Measured by Dynamic Enhanced MRI

Hon Yu, Min-Ying Su, Jun Wang, and Orhan Nalcioglu
Center for Functional Onco-Imaging, University of California, Irvine, CA 92697

Abstract

Chemotherapy induced longitudinal vascular changes taking place during the growth of R3230 AC adenocarcinoma were investigated using two contrast agents with different molecular weights, Gd-DTPA and Gadomer-17. Treated animals were separated into responders and partial-responders according their viable growth rate 3 weeks after the therapy. In responders a decrease in the vascular volume as well as in the vascular permeability were observed at 2-week post-therapy compared to 1-week's, whereas in controls an increase in both the vascular volume and permeability were observed at 2-week's compared to 1-week's as measured by Gadomer-17 using a pharmacokinetic model on a pixel-by-pixel basis, suggesting that vascular changes assessed by Gadomer-17 could serve as a tumor treatment monitor.

Purpose

Chemotherapy induced vascular and structural changes taking place in tumors were studied by using dynamic contrast enhanced MRI. In this study we investigated the longitudinal vascular changes occurring in tumors receiving Taxotere (an anti-angiogenic drug) treatment in order to find out if the vascular changes can serve as early indices that precede the structural changes (volumetric changes of viable region) in tumors' growth. In order to investigate the longitudinal vascular changes, we applied the dynamic contrast enhanced MRI with two different contrast agents, Gd-DTPA (<1 kD) and Gadomer-17 (35 kD), on the R3230 AC adenocarcinoma model. The baseline study was first performed then the animals received weekly taxotere treatment and weekly follow-up MRI studies. The measured enhancement kinetics of both contrast agents were analyzed with a pharmacokinetic model to derive parameters related to vascular volume (Vb) and permeability (K2) on a pixel-by-pixel basis. In each tumor the pixel population distribution curves of these two measured parameters and the volumetric changes in tumor size were calculated and the longitudinal changes in these two parameters were compared between the control and the treated groups to assess the differences between them.

Methods

Nine female Fisher-344 rats (160 ~ 170 g) bearing the R3230 AC adenocarcinomas were used in the study. When the tumor size grew to about 0.8 cm in diameter, the baseline study was conducted right after which six of the nine rats received the chemotherapy by injection of taxotere (4 mg/kg). At one (post-1), two weeks (post-2) and three weeks (post-3) after the baseline study the experiments were repeated and the rats in the treated group received the chemotherapy again after each MRI study. All of the MRI experiments were performed on a 3.0-T scanner using a Marconi console. The T2-weighted images covering across the tumor were acquired for volumetric measurements and a fast 3-D. Vol. T1-weighted dynamic sequence with TR/TE = 18/3.6 ms was used for the dynamic imaging with sequential injections of Gd-DTPA (0.1 mmol/kg), followed by Gadomer-17 (0.05 mmol/kg, a dendrimeric compound with size equivalent to 35 kD protein, provided by Schering AG, Berlin, Germany). The viable volumes, which were separated by the threshold segmentation from the total tumor volumes, measured at post-3 were normalized to their respective volumes measured at post-2 to calculate the viable growth ratio in each tumor. The enhancement kinetic from the viable region was measured and analyzed on a pixel-by-pixel basis by using a 2-compartmental model and the pixel population curves of Vb and K2 were obtained in each tumor. The longitudinal vascular changes in Vb and K2 were then compared between the control and the treated tumors.

Results

Three of the six treated rats were classified as the responder group as they showed a viable growth ratio of less than 1 (0.82, 0.88 and 0.88), whereas the other three treated rats were classified as partial responder group as their ratios were greater than 1 (1.07, 1.22 and 1.26), but still lower than the control group's (1.92, 1.93 and 2.24). The results obtained from analysis of the Gd-DTPA kinetics did not show any differences between the control and the treated groups and not presented here. Figures 1a and 1b show the pixel population distributions of Vb and K2, respectively, for the control group measured with Gadomer-17 at post-1 and post-2 which preceded the determination of the viable growth rate by one week. In the control group the curve at post-2 for Vb shows an increase throughout the whole population compared to the post-1's, whereas the distribution for K2 at post-2 shows an increase respect to its post-1's throughout the whole population. Figures 2a and 2b show the pixel population distributions at post-1 and post-2 measured with Gadomer-17 for Vb and K2 of the partial responder group, respectively. The partial responder group still shows an increase in Vb at post-2 respect to post-1's, but mostly in >50% pixel population range and shows a decrease in K2, mostly pronounced in >60% percentile range. The pixel population distribution curves of Vb and K2 for the responder group, which are shown in figures 3a and 3b, respectively, show a decrease in Vb in the entire population, and also show a decrease in K2, markedly in >50% percentile range, going from post-1 to post-2.

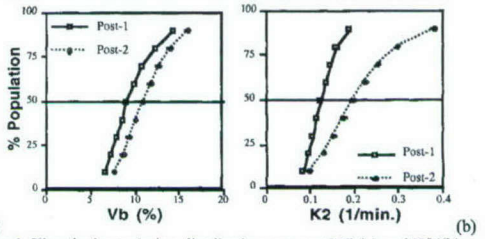

Figure 1. The pixel population distribution curves of Vb(a) and K2((b) from the control group.

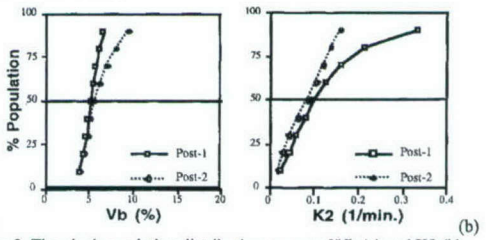

Figure 2. The pixel population distribution curves of Vb (a) and K2 (b) from the partial responder group.

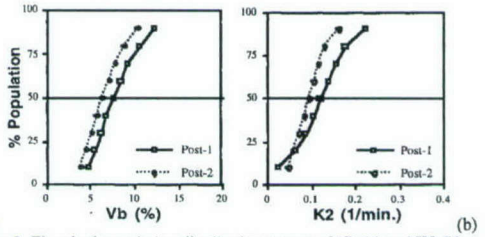

Figure 3. The pixel population distribution curves of Vb (a) and K2 (b) from the responder group.

Discussion

The vascular changes after the chemotherapy in this study as measured by Gadomer-17 seem to suggest that these changes could be used to predict the structural changes in tumor that would follow. The tumors in the responder group showed clearly different vascular changes at week-2 post the chemotherapy was initiated, which preceded the week-3 post time point when the viable growth ratio was determined to show the decrease in the viable volume, as measured by the parameters Vb and K2 compared to the control tumors' at the same time point. The results suggest that the early vascular changes in Vb and K2 as measured by Gadomer-17 could possibly serve to predict the treatment efficacy.

Acknowledgement

This work was supported in part by the US ARMY BCRP grant number DAMD17-01-0178.

Characterization of Carcinogen ENU Induced Benign and Malignant Mammary Tumors in Rats: Volumetric Growth Rates, Contrast Enhancement Kinetics, and Longitudinal Monitoring

Hon Yu, Min-Ying Su, Jun Wang, Phillip M. Carpenter[2], and Orhan Nalcioglu
Center for Functional Onco-Imaging, and [2]Department of Pathology, University of California-Irvine, CA, USA

Abstract

The carcinogen ENU could induce malignant tumors of various nuclear grades and different types of benign tumors, thus it can serve to investigate the sensitivity and specificity of experimental diagnostic agents for differential diagnosis and tumor staging. However, whether it can be used for studies of recurrence or metastasis has rarely been studied. We measured the volumetric growth rate and the enhancement kinetics of Gd-DTPA and Gadomer-17 for each tumor, and differences between malignant and benign tumors were investigated. Each tumor was surgically removed and the rats were kept for longitudinal monitoring for recurrence, development of other tumors, and metastasis.

Purpose

We performed a longitudinal study to characterize carcinogen ENU induced mammary tumor model. ENU can induce benign and malignant tumors in rats, and the malignant tumors came with various SBR (Scarff-Bloom-Richardson) grades, thus it can be used a suitable model for studies of differential diagnosis between benign and malignant tumors as well as malignant tumor grade staging. For each tumor 2 MRI studies were performed. The volumetric growth rates were calculated from the sizes measured in these two studies. The enhancement kinetics of two contrast agents, the small agent Gd-DTPA and a mid-sized agent Gadomer-17, were measured. The volumetric growth rates, as well as the early (30-sec) and maximum (approximately 2-min) enhancements between benign and malignant tumors were compared. Each tumor was surgically removed and the rats were kept for observation of recurrence, further development of other tumors, and metastasis into other organs, to explore whether this model can be used to study recurrence and metastasis as in human breast cancer.

Methods

N-ethyl-N-nitrosourea (ENU, 90 mg/kg) was injected i.p. into 30-day old SPF Sprague-Dawley rats (n=50) to induce mammary tumors [Stoica et al. Anticancer Research 4:5, 1984]. The tumors started to appear 2 months after injection. The baseline MRI study was performed when the tumor reached approximately 1.0 cm in diameter. The experiments were performed on a home-built 3.0 T scanner with technical support provided by Marconi Inc. The protocol included a T2-weighted fast spin echo sequence (TR/TE= 3000/105 ms, echo train=8, FOV=14 cm, 2-mm slice) covering the entire tumor for volumetric measurement, and dynamic contrast enhanced studies using two agents, Gd-DTPA (0.1 mmol/kg) and Gadomer-17 (0.05 mmol/kg). Gadomer-17 was provided by Schering AG (Berlin, Germany), which is a synthetic dendrimeric gadolinium chelate with an apparent molecular weight of 35 kD. The dynamic images were acquired by using a 3D gradient echo pulse sequence with TR/TE=18/3.6 ms, flip angle=20°, FOV=10.5, 5-mm thickness). Gd-DTPA was injected first, and 1 hour later Gadomer-17 was injected. In 1-3 weeks when the tumor size was approximately doubled, the follow-up MRI study was performed. Only the T2-weighted sequence was performed to measure the tumor volume. The volumetric growth rates were expressed in cc/day. The early and maximum enhancements at 30-sec and 2-min after contrast administration was measured. After the imaging studies were finished, the tumor was surgically removed for pathological examination. The rats were kept alive for observation of recurrence or development of additional tumors. If more tumors were found, the same baseline and follow-up MRI studies were performed again. Rats were euthanized when there were tumors found in the abdomen. The abdominal tumor was also removed for pathological examination to determine whether it was a metastasis from the mammary tumor or it was from a different origin.

Results

Ninety three tumors were found in 1 year after the injection of ENU. Most tumors belonged to four major types, 2 malignant and 2 benign. The malignant tumors included ductal adenocarcinoma (n=25) and papillary adenocarcinoma (n=21), and the two major benign lesions were fibroadenoma (n=24) and adenosis (n=13). Multiple tumors (up to 5) could develop in one rat, all at different locations. Interestingly no tumor recurrence was observed at the surgical site after removal of a previous tumor. Also, none of the abdominal tumors were from breast origin. We also investigated lymph nodes from some rats, and found no sign of any cancer. The growth rates and the early (30 sec) and maximum (2-min) enhancements measured by Gd-DTPA and Gadomer-17 are listed in table 1. The bar graphs are shown in Figure 1. The two malignant tumors exhibited similar enhancement kinetics, showing rapid early enhancing slope and high enhancement magnitude. The two benign lesions had much slower early enhancing slope (highly significantly). However, adenosis could reach to a higher enhancement at 2-min after contrast administration, almost comparable to that in malignant tumors. The enhancements at 2-min between fibroadenoma and malignant tumors also became closer, but still significantly different.

Table 1: Growth Rate & Enhancements in 4 tumor types

	Papillary AC	Ductal AC	Adenosis	FA
GR (cc/day)	0.07 ± 0.14	0.06 ± 0.13	0.05 ± 0.06	0.03 ± 0.03
Gd-DTPA 30s	126 ± 68	122 ± 62	57 ± 22	39 ± 14
Gd-DTPA 2min	240 ± 75	251 ± 69	204 ± 65	145 ± 54
Gadomer17 30s	52 ± 23	47 ± 30	24 ± 11	23 ± 10
Gadomer17 2min	96 ± 32	92 ± 40	73 ± 22	51 ± 19

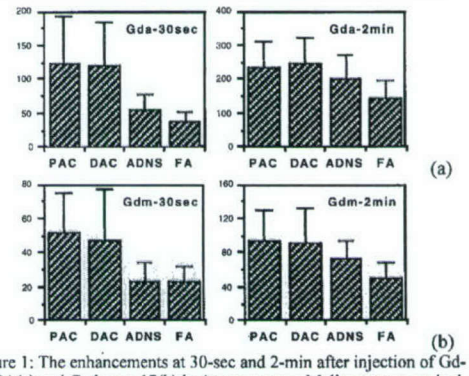

Figure 1: The enhancements at 30-sec and 2-min after injection of Gd-DTPA(a) and Gadomer-17(b) in 4 tumor types. Malignant tumors had higher early enhancements. Results measured by both agents were similar.

Discussion

The carcinogen ENU induced benign and malignant tumors, thus this animal tumor model was suitable for studies of experimental diagnostic agents. A better characterization of this model is needed. Our results demonstrated that all developed tumors were primary tumors, and they did not metastasize to lymph nodes or to other organs. The growth rates showed large variations even within each tumor type, and they were not correlated with the enhancement kinetics of both studied contrast agents. As in human breast tumors, the early enhancement is the best parameter to differentiate benign from malignant tumors.

Acknowledgement

This work was supported in part by NIH grant # R21 CA86215.